J. Fluid Mech. (2006), *vol.* 568, *pp.* 387–424.
doi:10.1017/S0022112006002448 Printed in the United Kingdom

Viscous–inviscid interaction in transonic Prandtl–Meyer flow

By A. I. RUBAN[1], X. WU[2,3] AND R. M. S. PEREIRA[4]

[1]School of Mathematics, University of Manchester, Oxford Road, Manchester M13 9PL, UK

[2]Department of Mathematics, Imperial College London, 180 Queen's Gate, London SW7 2AZ, UK

[3]Department of Mechanics, Tianjin University, China

[4]Universidade do Minho, Dept Mathematica para Ciencia e Tecnologia, 4800-058 Guimaraes, Portugal

(Received 26 August 2005 and in revised form 22 May 2006)

This paper presents a theoretical analysis of perfect gas flow over a convex corner of a rigid-body contour. It is assumed that the flow is subsonic before the corner. It accelerates around the corner to become supersonic, and then undergoes an additional acceleration in the expansion Prandtl–Meyer fan that forms in the supersonic part of the flow behind the corner. The entire process is described by a self-similar solution of the Kármán–Guderley equation. The latter shows that the boundary layer approaching the apex of the corner is exposed to a singular pressure gradient, $\mathrm{d}p/\mathrm{d}x \sim (-x)^{-3/5}$, where x denotes the coordinate measured along the body surface from the corner apex. Under these conditions, the solution for the boundary layer also develops a singularity. In particular, the longitudinal velocity near the body surface behaves as $U \sim Y^{1/2}$. Here Y is the normal coordinate scaled with the boundary-layer thickness $Re^{-1/2}$; Re being the Reynolds number, assumed large in this theory.

As usual, the boundary layer splits up into two parts, a viscous near-wall sublayer and a locally inviscid main part of the boundary layer. The analysis of the displacement effect of the boundary layer shows that neither the viscous sublayer nor the main part determines the displacement thickness. Instead, the overlapping region situated between them proves to be responsible for the shape of the streamlines at the outer edge of the boundary layer. This leads to a significant simplification of the analysis of the flow behaviour in the viscous–inviscid interaction region that forms in a small vicinity of the corner. In order to describe the flow behaviour in this region, one has to solve the Kármán–Guderley equation for the inviscid part of the flow outside the boundary layer. The influence of the boundary layer is expressed through a boundary condition, that relates the streamline deflection angle ϑ at the outer edge of the boundary layer to the pressure gradient $\mathrm{d}p/\mathrm{d}x$ acting upon the boundary layer. The boundary-layer analysis leads to an analytical formula that relates ϑ and $\mathrm{d}p/\mathrm{d}x$ (unlike in previous studies of the viscous–inviscid interaction). The interaction problem was solved numerically to confirm that the solution develops a finite-distance singularity.

1. Introduction

The flow near a corner of a rigid-body contour represents an example where the hierarchical strategy of the classical boundary-layer theory of Prandtl (1904) ceases

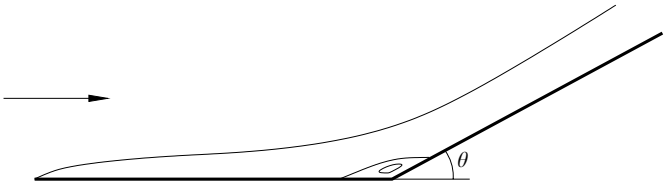

FIGURE 1. Subsonic/supersonic flow past a corner.

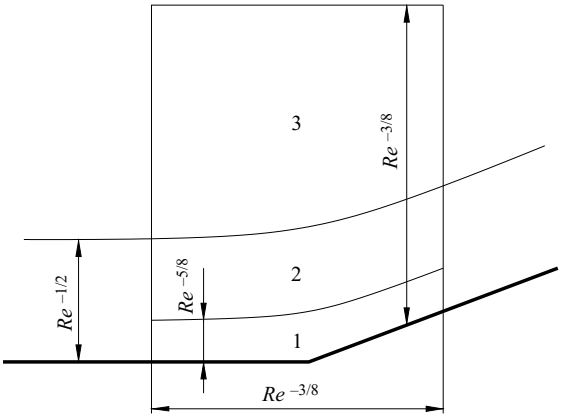

FIGURE 2. Three-tiered structure of the interaction region.

to be applicable. Instead, the theory of viscous–inviscid interaction should be used. It was developed independently by Neiland (1969*a*) and Stewartson & Williams (1969) for supersonic flow separating from a smooth body surface and by Stewartson (1969) and Messiter (1970) for incompressible fluid flow past the trailing edge of a flat plate. Theoretical investigations of the flow over corners started immediately after that. In 1970, Stewartson conjectured that the incipience of separation, both in subsonic and supersonic flows, takes place when the angle θ swept by the tangent to the body contour at the corner point (see figure 1) is an $O(Re^{-1/4})$ quantity, where Re is the Reynolds number.

Based on the asymptotic analysis of the Navier–Stokes equations at large values of Re, Stewartson demonstrated that a small vicinity of the corner is occupied by the region of interaction between the boundary layer and external inviscid flow. This region is $O(Re^{-3/8})$ long and has a three-tiered structure (see figure 2) being composed of the viscous near-wall sublayer (region 1), the main part of the boundary layer (region 2) and an inviscid potential flow (region 3) situated outside the boundary layer.

The characteristic width of the viscous sublayer is estimated as being an $O(Re^{-5/8})$ quantity, so that it occupies an $O(Re^{-1/8})$ portion of the boundary layer and is comprised of the stream filaments immediately adjacent to the wall. The flow velocity in this region is $O(Re^{-1/8})$ relative to the free-stream velocity, and owing to the slow motion of the fluid here, the flow exhibits high sensitivity to pressure variations. Even a small pressure rise along the wall may cause significant deceleration of fluid particles there. This leads to thickening of flow filaments, and the streamlines change their shape, being displaced from the wall.

The middle tier of the interactive structure represents a continuation of the conventional boundary layer. Its thickness is thus $O(Re^{-1/2})$, and the velocity is

an $O(1)$ quantity. The flow in this tier is significantly less sensitive to the pressure variations. It does not produce any noticeable contribution to the displacement effect of the boundary layer, which means that all the streamlines in the middle tier are parallel to each other and carry the deformation produced by the displacement effect of the viscous sublayer.

Finally, the upper tier is situated in the potential flow region outside the boundary layer. It serves to 'convert' the perturbation in the form of the streamline deflection into a perturbation of pressure. The latter is then transmitted through the main part of the boundary layer back to the sublayer.

For the separation to take place, a certain level of perturbation is necessary. It is reached when the scaled ramp angle $\theta_0 = Re^{1/4}\theta$ assumes a critical value. In order to describe the flow behaviour in the interaction region, one needs to use the Prandtl boundary-layer equations for region 1,

$$u\frac{\partial u}{\partial x} + v\frac{\partial u}{\partial y} = -\frac{\mathrm{d}p}{\mathrm{d}x} + \frac{\partial^2 u}{\partial y^2}, \tag{1.1}$$

$$\frac{\partial u}{\partial x} + \frac{\partial v}{\partial y} = 0. \tag{1.2}$$

These have to be solved with the no-slip condition on the ramp surface

$$u = v = 0 \quad \text{at} \quad y = 0, \tag{1.3}$$

and the matching conditions with the solutions in the boundary layer upstream of the interaction region

$$u = y \quad \text{at} \quad x = -\infty \tag{1.4}$$

and in the middle tier (region 2)

$$u \to y + A(x) + \cdots \quad \text{as} \quad y \to \infty. \tag{1.5}$$

Function $A(x)$ in (1.5) determines the shape of the streamlines in the main part of the boundary layer, and for this reason is termed the displacement function. Using (1.5) in (1.2) it may be easily deduced that at the outer edge of the viscous sublayer $v/u = -\mathrm{d}A/\mathrm{d}x$. As the deformation of the streamlines, produced by the viscous sublayer, remains unchanged across the middle tier (region 2), we can conclude that at the 'bottom' of the upper tier (region 3) the slope of the streamlines is given by $\vartheta = -\mathrm{d}A/\mathrm{d}x + \mathrm{d}f/\mathrm{d}x$. Here in addition to the displacement effect of the boundary layer, the contribution of the body shape is taken into account. Function $f(x)$ which represents the body shape is written near the corner point as

$$f(x) = \begin{cases} 0 & \text{if} \quad x < 0, \\ \theta_0 x & \text{if} \quad x < 0. \end{cases}$$

Here θ_0 might be either positive or negative, which corresponds to concave and convex corners, respectively.

In order to determine the response of the inviscid flow outside the boundary layer to the displacement effect, one has to analyse the flow in region 3. Here the thin aerofoil theory is applicable. It allows the formulation of the so called 'interaction law' which relates the induced pressure p to the displacement function A. In the case of a supersonic flow it is given by Ackeret's formula

$$p = -\frac{\mathrm{d}A}{\mathrm{d}x} + \frac{\mathrm{d}f}{\mathrm{d}x}. \tag{1.6a}$$

For a subsonic flow, it should be substituted by the Hilbert integral

$$p = -\frac{1}{\pi}\int_{-\infty}^{\infty} \frac{\mathrm{d}A/\mathrm{d}s - \mathrm{d}f/\mathrm{d}s}{s-x}\mathrm{d}s. \tag{1.6b}$$

In his original work, Stewartson (1970) concentrated on the solution of the linearized version of the interaction problem (1.1)–(1.6). The latter is applicable in the case when $\theta_0 \ll 1$, for which the corner merely causes a small perturbation to the boundary layer that will remain attached to the body surface. The first numerical solution of the full nonlinear problem was conducted by Jenson, Burggraf & Rizzetta (1975) for supersonic flow and by Ruban (1976) for subsonic flow. Since then the problem has been revisited on numerous occasions. Numerical results may be found in Korolev (1991, 1992) for subsonic flows and in Korolev, Gajjar & Ruban (2002) supersonic flows. The results of the calculations show that the subsonic flow separates both at concave ($\theta > 0$) and convex ($\theta < 0$) corners with the critical values of θ_0 being 2.51 and -5.21, respectively. The supersonic flow separates only when the corner is concave. This happens as soon as θ_0 reaches a critical value of 1.57.

Large-scale separation of subsonic flow from a convex corner, that is observed when θ in figure 1 is an order one negative quantity, was studied by Ruban (1974). He found that in the limit when $Re \to \infty$, the flow may be described by the Kirchhoff (1869) model with the so called 'free streamline' emanating from the corner point. The presence of the separation region influences the pressure field in such a way that the pressure gradient acting on the boundary layer before the corner develops a singularity,

$$\frac{\mathrm{d}p}{\mathrm{d}x} = -\frac{\kappa}{(-x)^{1/2}} + \cdots \quad \text{as} \quad x \to 0^-. \tag{1.7}$$

Here, x is a coordinate measured along the body contour from the corner point, and κ is a positive $O(1)$ constant. As a result of this singularity, the velocity profile in the boundary layer approaching the separation region changes significantly, which in turn leads to a shortening of the interaction region. Instead of being $O(Re^{-3/8})$ long (see figure 2), its longitudinal scale changes to $O(Re^{-4/9})$. Still, the interaction process remains in essence the same as in the starndard triple-deck theory, with the lower tier generating the main contribution into the displacement effect, whilst the upper tier acts to convert it into a pressure perturbation.

The transonic version of this problem was considered by Ruban & Turkyilmaz (2000). They found that when the gas speed at the separation point coincides with the speed of sound, the pressure gradient upstream of the interaction region becomes even stronger, that is,

$$\frac{\mathrm{d}p}{\mathrm{d}x} = -\frac{\kappa}{(-x)^{2/3}} + \cdots \quad \text{as} \quad x \to 0^-. \tag{1.8}$$

This leads to a drastic change in the physical nature of the processes taking place in the interaction region. Ruban & Turkyilmaz (2000) found that in this case, the displacement of the boundary layer is produced mainly by the middle tier (region 2 in figure 2) where the flow is inviscid. Consequently, the interaction process takes place between the middle and upper tiers, and therefore, may be called *inviscid–inviscid*.

Experimental observations show that unlike incompressible fluid flows which always separate from a convex corner, a perfect gas flow may assume two different forms. The first one is a flow with separation from the corner point; it was considered earlier by Ruban & Turkyilmaz (2000). The second possibility is that the flow remains fully

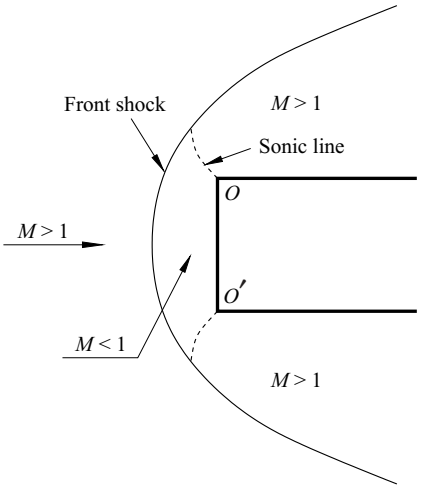

FIGURE 3. Supersonic flow past a flat-faced plate.

attached to the body contour. It forms naturally in various physical situations (see photographs 262–264 in Van Dyke 1982). A typical example is sketched in figure 3. It reproduces figure 3.17.7 in Cherny (1988) and summarizes numerous numerical simulations of the flow based on the inviscid calculations of various authors. Here, a supersonic flow with a Mach number $M > 1$ approaches a flat-faced plate. The flow remains unperturbed everywhere before the bow shock wave that forms in front of the plate. The shock causes the gas to lose its speed abruptly, and this results in the subsonic flow region ($M < 1$) between the shock and body face. The gas then flows round the corners O and O'. For incompressible fluid, the classical inviscid flow theory predicts an unbounded velocity near a convex corner, and this result is traditionally used to argue that an attached incompressible flow round a corner is physically impossible.

Contrary to that, a gas can reach only a finite speed. It first accelerates to the so-called 'sonic line' where the gas speed coincides with the local speed of sound, and Mach number $M = 1$. The sonic line originates from the corner point and separates the subsonic part of the flow from supersonic. Downstream of the sonic line the flow experiences an additional acceleration in the Prandtl–Meyer expansion fan. Our task in this paper is first to show that Prandtl–Meyer fan may occur near a corner point in a variety of body shapes, and then to study the viscous–inviscid interaction region that forms near the corner point.

2. Properties of the inviscid transonic flow

We assume that locally near point O the body surface has a shape as shown in figure 4, i.e. it is flat upstream of point O, and bends up or down downstream of this point. The curvature of the body contour is discontinuous at point O, which may be viewed as a 'corner' even though the contour itself may be smooth.

It is well known that any two-dimensional steady inviscid flow of a perfect gas satisfies the equation (see, for example, Cole & Cook 1986)

$$(\hat{a}^2 - \hat{u}^2)\frac{\partial \hat{u}}{\partial \hat{x}} + (\hat{a}^2 - \hat{v}^2)\frac{\partial \hat{v}}{\partial \hat{y}} = \hat{u}\hat{v}\left(\frac{\partial \hat{v}}{\partial \hat{x}} + \frac{\partial \hat{u}}{\partial \hat{y}}\right). \tag{2.1}$$

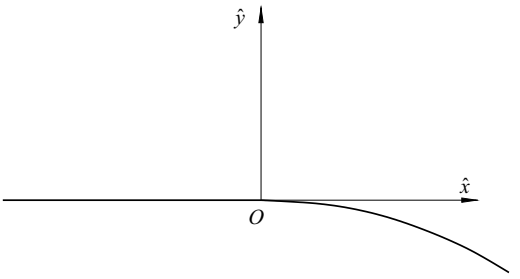

FIGURE 4. Geometrical layout of the flow.

Here $\hat{x}$, $\hat{y}$ are Cartesian coordinates and $\hat{u}$, $\hat{v}$ are velocity components with respect to these coordinates. The 'hat' signifies a dimensional variable. For our purposes, it is convenient to choose the coordinate system in such a way that the origin coincides with point O and the $\hat{x}$-axis is directed along the tangent to the body surface upstream of this point.

The speed of sound is denoted in equation (2.1) by $\hat{a}$. Its value at each point of the flow field is related to the velocity components via the Bernoulli equation

$$\frac{\hat{a}^2}{\gamma-1}+\frac{\hat{u}^2+\hat{v}^2}{2}=\frac{\hat{a}_\infty^2}{\gamma-1}+\frac{\hat{V}_\infty^2}{2}, \tag{2.2}$$

where γ is the ratio of specific heats, $\hat{V}_\infty$ is the gas velocity in the unperturbed flow upstream of the body and $\hat{a}_\infty$ denotes the corresponding value of the speed of sound.

If the flow (in the local region of interest) is free of shock waves, or shock waves are weak, which is always the case in the transonic regime, then it may be treated as irrotational,

$$\frac{\partial\hat{u}}{\partial\hat{y}}-\frac{\partial\hat{v}}{\partial\hat{x}}=0, \tag{2.3}$$

and there exists a potential function $\hat{\Phi}(\hat{x},\hat{y})$ such that

$$\hat{u}=\frac{\partial\hat{\Phi}}{\partial\hat{x}}, \qquad \hat{v}=\frac{\partial\hat{\Phi}}{\partial\hat{y}}. \tag{2.4}$$

Once the solution of equations (2.1)–(2.4) is found, one can determine the pressure $\hat{p}$ and density $\hat{\rho}$ at each point in the flow field using the Bernoulli equation (2.2), rewritten in the form

$$\frac{\gamma}{\gamma-1}\,\frac{\hat{p}}{\hat{\rho}}+\frac{\hat{u}^2+\hat{v}^2}{2}=\frac{\gamma}{\gamma-1}\,\frac{\hat{p}_\infty}{\hat{\rho}_\infty}+\frac{\hat{V}_\infty^2}{2}, \tag{2.5}$$

and the entropy conservation law

$$\frac{\hat{p}}{\hat{\rho}^\gamma}=\frac{\hat{p}_\infty}{\hat{\rho}_\infty^\gamma}. \tag{2.6}$$

Let the gas velocity, density and pressure at point O be denoted by $\hat{V}_0$, $\hat{\rho}_0$ and $\hat{p}_0$, respectively. Using these quantities we introduce the non-dimensional variables,

$$\left.\begin{array}{lll}\hat{u}=\hat{V}_0u, & \hat{v}=\hat{V}_0v, & \hat{\Phi}=\hat{V}_0L\Phi,\\ \hat{a}=\hat{V}_0a, & \hat{\rho}=\hat{\rho}_0\rho, & \hat{p}=\hat{p}_0+\hat{\rho}_0\hat{V}_0^2p,\\ & \hat{x}=Lx, & \hat{y}=Ly.\end{array}\right\} \tag{2.7}$$

Here, L is the characteristic dimension of the body. In what follows, we shall assume that $\hat{V}_0$ coincides with the speed of sound $\hat{a}_0$ at point O. In essence the requirement, $\hat{V}_0 = \hat{a}_0$, represents the transonic flow assumption. The ensuing analysis is concerned with a locally transonic flow, which can be 'embedded' in a complex global flow (such as that shown in figure 3). The latter may be supersonic and may even consist of shocks.

Substitution of (2.7) into (2.1)–(2.4) gives

$$\left(a^2 - u^2\right)\frac{\partial u}{\partial x} + \left(a^2 - v^2\right)\frac{\partial v}{\partial y} = uv\left(\frac{\partial v}{\partial x} + \frac{\partial u}{\partial y}\right), \tag{2.8}$$

$$u = \frac{\partial \Phi}{\partial x}, \quad v = \frac{\partial \Phi}{\partial y}, \tag{2.9}$$

$$\frac{a^2}{\gamma - 1} + \frac{u^2 + v^2}{2} = \frac{1}{\gamma - 1} + \tfrac{1}{2}. \tag{2.10}$$

The Bernoulli equation (2.5) and entropy conservation law (2.6), written in non-dimensional variables, take the form

$$\frac{u^2 + v^2}{2} + \frac{1}{(\gamma - 1)\rho} + \frac{\gamma}{\gamma - 1}\frac{p}{\rho} = \tfrac{1}{2} + \frac{1}{(\gamma - 1)}, \tag{2.11}$$

$$1 + \gamma p = \rho^{\gamma}. \tag{2.12}$$

In order to formulate the boundary conditions which should be applied when solving equations (2.8)–(2.10), we shall write the equation for the body contour as

$$y = Y_b(x).$$

Then the impermeability condition on the body surface requires that

$$\frac{v}{u} = Y_b'(x) \quad \text{at} \quad y = Y_b(x). \tag{2.13}$$

2.1. *Self-similar solution*

Let us assume that near point O,

$$Y_b(x) = \begin{cases} 0, & x < 0, \\ a_0 x^{\alpha}, & x > 0, \end{cases} \tag{2.14}$$

where constant a_0 might be positive or negative so that the wall may bend up or down. In what follows, parameter α is assumed to belong to the interval

$$\alpha \in (1, 2) \tag{2.15}$$

such that the tangent to the body contour remains continuous, but the curvature is discontinuous and infinite at point O. In the rest of this section, we shall show that a local similarity solution satisfying both upstream and downstream boundary conditions may be constructed for each $\alpha \in (1, 8/5)$, with $\alpha = 8/5$ being the singular limit. The relevance of the solution for the limiting case to the flow shown in figure 3 will be discussed at the end of this section.

Since no characteristic length scale can be ascribed to the body shape (2.14), the solution of the problem (2.8)–(2.10), (2.13) can be sought (in a small vicinity of point O) in a self-similar form. For the velocity potential $\Phi(x, y)$, we use the coordinate asymptotic expansion

$$\Phi(x, y) = x + \frac{1}{\gamma + 1} y^{3k-2} F_0(\xi) + \cdots \quad \text{as} \quad y \to 0. \tag{2.16}$$

The first term on the right-hand side of (2.16) is chosen such that it gives the velocity vector that is tangential to the body contour at point O and has a unit modulus as required by the first of the non-dimensionalization formulae (2.7). Function $F_0(\xi)$ in the next term depends on the similarity variable

$$\xi = \frac{x}{y^k} \tag{2.17}$$

which is supposed to remain $O(1)$ as x and y simultaneously tend to zero. The $(3k-2)$ power of y is chosen so that the dominant terms balance in (2.8). For the remaining terms to be smaller, parameter k must be greater than one, but is otherwise undefined at this stage.

Substitution of (2.16) and (2.17) into (2.9) yields

$$u = 1 + \frac{1}{\gamma+1} y^{2k-2} F_0'(\xi) + \cdots, \tag{2.18}$$

$$v = \frac{1}{\gamma+1} y^{3k-3} [(3k-2)F_0(\xi) - k\xi F_0'(\xi)] + \cdots. \tag{2.19}$$

Note that $u \to 1$ and $v \to 0$ as $y \to 0$ since $k > 1$.

Now use of (2.18), (2.19) in the Bernoulli equation (2.10), gives the local sound speed as

$$a = 1 - \frac{(\gamma-1)}{2(\gamma+1)} y^{2k-2} F_0'(\xi) + \cdots. \tag{2.20}$$

Using further (2.18) and (2.19) to calculate $(u^2 + v^2)$ in (2.11) and then solving equations (2.11), (2.12) for p and ρ, we find

$$\left.\begin{aligned} p &= -\frac{1}{\gamma+1} y^{2k-2} F_0'(\xi) + \cdots \\ \rho &= 1 - \frac{1}{\gamma+1} y^{2k-2} F_0'(\xi) + \cdots \end{aligned}\right\} \quad \text{as } y \to 0. \tag{2.21}$$

Notice that asymptotic expansions (2.18)–(2.21) are applicable in situations which are not transonic as a whole but involve an $O(1)$ Mach number variation, like the flow shown in figure 3, where the Much number is zero at the front stagnation point, but increases to one as the corner points O and O' are approached. Of course, it follows from (2.18) and (2.20) that the Mach number is close to one near the corner points.

Now our task is to determine function $F_0(\xi)$. Substituting (2.18) and (2.19) together with (2.20) into (2.8) and setting $y \to 0$, we arrive at the equation for $F_0(\xi)$,

$$(F_0' - k^2\xi^2)F_0'' - k(5-5k)\xi F_0' + (3-3k)(3k-2)F_0 = 0. \tag{2.22}$$

Boundary conditions for this equation may be deduced from the impermeability condition (2.13). We note that near the body surface upstream of point O, the similarity variable (2.17) is large and negative. As shown in Ruban & Turkyilmaz (2000) the corresponding asymptotic solution of equation (2.22) may be written in the form

$$F_0(\xi) = d_0(-\xi)^{3-2/k} + d_1(-\xi)^{3-3/k} + \cdots \quad \text{as} \quad \xi \to -\infty, \tag{2.23}$$

where d_0 and d_1 are constants. Substitution of (2.23) into (2.19) yields

$$v = \frac{d_1}{\gamma+1}(-x)^{3-3/k} + \cdots \quad \text{as} \quad x \to 0^-.$$

Since the body surface is assumed to be flat upstream of point O, the impermeability condition (2.13) reduces to

$$v\Big|_{y=0} = 0,$$

and we see that

$$d_1 = 0. \tag{2.24}$$

Similarly, downstream of point O,

$$F_0(\xi) = b_0\xi^{3-2/k} + b_1\xi^{3-3/k} + \cdots \quad \text{as} \quad \xi \to +\infty. \tag{2.25}$$

Substitution of (2.25) into (2.18) and (2.19) yields

$$u = 1 + \frac{1}{\gamma+1}\left[b_0\Big(3-\frac{2}{k}\Big)x^{2-2/k} + b_1\Big(3-\frac{3}{k}\Big)yx^{2-3/k} + \cdots\right], \tag{2.26}$$

$$v = \frac{b_1}{\gamma+1}\,x^{3-3/k} + \cdots. \tag{2.27}$$

Now we can substitute (2.26), (2.27) together with (2.14) into the impermeability condition (2.13). We find that parameter k in the self-similar solution (2.16), (2.17) is related to parameter α in the equation for the body contour (2.14) as

$$k = \frac{3}{4-\alpha}, \tag{2.28}$$

and the second coefficient b_1 in the asymptotic expansion (2.25) is related to the factor a_0 in (2.14) as

$$b_1 = \alpha(\gamma+1)a_0. \tag{2.29}$$

Equation (2.22), considered with the upstream (2.23), (2.24) and downstream (2.25), (2.29) conditions, constitutes a boundary-value problem for function $F_0(\xi)$. It may be easily converted into an initial-value problem because equation (2.22) admits the invariant transformation

$$\xi \longrightarrow \Lambda\xi, \qquad F_0 \longrightarrow \Lambda^3 F_0, \tag{2.30}$$

with Λ being an arbitrary constant. This means that without loss of generality one can choose d_0 in (2.23) to be $d_0 = 1$ for all positive d_0, and $d_0 = -1$ for all negative d_0. We shall concentrate here on the former case. It corresponds to the flow which is subsonic upstream of point O, but accelerates as this point is approached. Indeed, substitution of (2.23) into (2.18) yields to the leading order

$$u = 1 - \frac{d_0}{\gamma+1}\Big(3-\frac{2}{k}\Big)(-x)^{2-2/k} + \cdots \quad \text{as} \quad x \to 0^-.$$

It follows from 2.28 that corresponding to (2.15) the range of variation of k is $\big(1, 3/2\big)$, and we see that $u < 1$ for all $d_0 > 0$.

In view of condition (2.24), the second term in (2.23) vanishes, and after calculating the next-order term we have

$$F_0(\xi) = (-\xi)^{3-2/k} + \frac{(3k-2)^2(1-k)}{k^3}\,(-\xi)^{3-4/k} + \cdots \quad \text{as} \quad \xi \to -\infty. \tag{2.31}$$

This formula was used in our calculations to determine the initial conditions for F_0 and F_0' at the left-hand side boundary $\xi = \xi_{min}$ of the computational domain $\xi \in [\xi_{min}, \xi_{max}]$. Equation (2.22) was then integrated numerically from $\xi = \xi_{min}$ towards

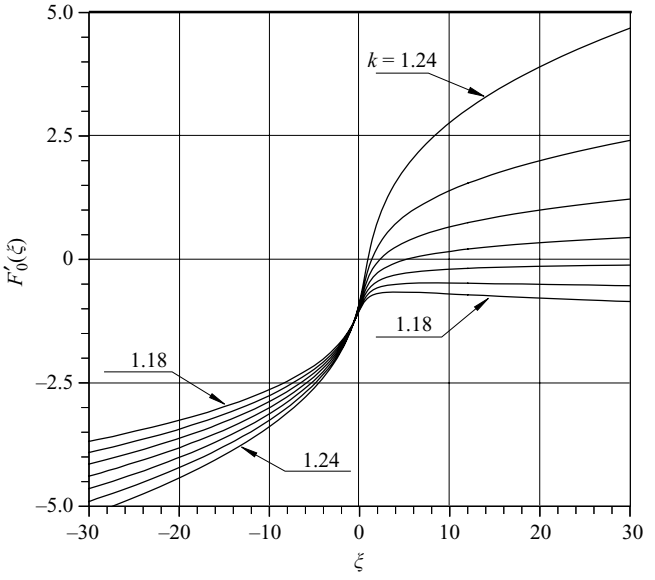

FIGURE 5. Results of the numerical solution of equation (2.22) for $k = 1.18$ through $k = 1.24$ with the interval $\Delta k = 0.01$.

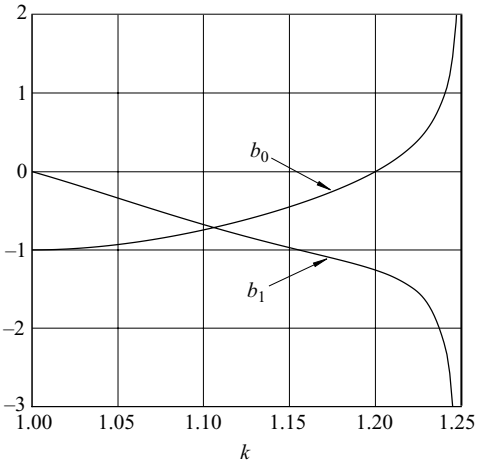

FIGURE 6. The behaviour of the coefficients b_0 and b_1 of the asymptotic expansion (2.25).

$\xi = \xi_{max}$ for different values of k. A number of computational domains were tried; the largest was $[-70, 70]$. A uniform mesh was used throughout this study with up to 2000 node points between $\xi = \xi_{min}$ and $\xi = \xi_{max}$. The results proved to be mesh independent to the graphic accuracy, and are presented in figures 5 and 6. Figure 5 displays the derivative of function $F_0(\xi)$. Formula (2.18) shows that the flow is subsonic as long as $F_0'(\xi)$ remains negative, and turns into supersonic when $F_0'(\xi)$ becomes positive. Notice that for all $k < 6/5$, the flow first accelerates and then, after $F_0'(\xi)$ reaches a maximum, starts to decelerate slightly; it remains subsonic in the entire interval $\xi \in (-\infty, \infty)$. Monotonic increase of $F_0'(\xi)$ is first observed at $k = 6/5$ when the gas velocity tends to the speed of sound as $\xi \to \infty$. For larger values of

k, the flow acceleration leads to the formation of a supersonic region beyond some value of ξ.

Figure 6 shows the behaviour of coefficients b_0 and b_1 in the downstream asymptotic expansion (2.25). We see that b_0 becomes zero at $k = 6/5$. Hence, for this value of k, expansion (2.25) is written as

$$F_0(\xi) = b_1 \xi^{1/2} + \cdots \quad \text{as} \quad \xi \to \infty,$$

and therefore the derivative

$$F_0'(\xi) = \tfrac{1}{2} b_1 \xi^{-1/2} + \cdots \quad \text{as} \quad \xi \to \infty$$

really tends to zero as figure 5 suggests.

The solution develops a singularity at $k = 5/4$ when both b_0 and b_1 become infinite. We were unable to find solutions to equation (2.22) with initial condition (2.31) for $k \geqslant 5/4$.

2.2. *Phase portrait*

In order to understand better what happens when k approaches 5/4, we shall study the solution in a phase plane (see Buldakov & Ruban 2002). Guided by (2.18) and (2.19), we represent the velocity components in the form

$$\left.\begin{aligned} u &= 1 + \frac{1}{\gamma+1} y^{2k-2} F(\xi) + \cdots \\ v &= \frac{1}{\gamma+1} y^{3k-3} G(\xi) + \cdots \end{aligned}\right\} \quad \text{as} \quad y \to 0. \tag{2.32}$$

Asymptotic expansion (2.20) for the speed of sound is now written as

$$a = 1 - \frac{(\gamma-1)}{2(\gamma+1)} y^{2k-2} F(\xi) + \cdots \quad \text{as} \quad y \to 0. \tag{2.33}$$

Equations for $F(\xi)$ and $G(\xi)$

$$\frac{\mathrm{d}F}{\mathrm{d}\xi} = (k-1)\frac{3G - 2k\xi F}{F - k^2\xi^2}, \quad \frac{\mathrm{d}G}{\mathrm{d}\xi} = (k-1)\frac{2F^2 - 3k\xi G}{F - k^2\xi^2}, \tag{2.34}$$

may be deduced by substituting (2.32)–(2.33) into (2.8) and the irrotation condition (2.3), Alternatively, we can see that

$$F(\xi) = F_0'(\xi), \qquad G(\xi) = (3k-2)F_0(\xi) - k\xi F_0'(\xi), \tag{2.35}$$

and deduce equations (2.34) by manipulating (2.22).

Invariant transformation (2.30) is now written as

$$\xi \longrightarrow \Lambda\xi, \qquad F \longrightarrow \Lambda^2 F, \qquad G \longrightarrow \Lambda^3 G.$$

In order to make the solution independent on the group parameter Λ, one can introduce instead of $F(\xi)$ and $G(\xi)$ new functions $f(\xi)$ and $g(\xi)$

$$f(\xi) = \frac{F(\xi)}{k^2\xi^2}, \qquad g(\xi) = \frac{G(\xi)}{k^3\xi^3}. \tag{2.36}$$

Now each trajectory in the (f, g)-phase plane will represent a family of solutions for all possible values of Λ. Introducing further a new independent variable χ such that

$$\mathrm{d}\chi = \frac{\mathrm{d}\xi}{(f-1)k\xi}, \tag{2.37}$$

we arrive at the following non-singular autonomous system

$$\left.\begin{aligned}\frac{\mathrm{d}f}{\mathrm{d}\chi} &= 2f + 3(k-1)g - 2kf^2,\\ \frac{\mathrm{d}g}{\mathrm{d}\chi} &= 2(k-1)f^2 - 3kfg + 3g.\end{aligned}\right\} \tag{2.38}$$

The independent variable transformation (2.37) divides the phase plane into two sheets, one for $\xi < 0$ and another for $\xi > 0$. The latter differs from the former only by the direction of change of the original coordinate ξ with respect to the new coordinate χ. Each of the sheets has a singular line $f = 1$ where ξ changes its direction as well. An intersection of this line by a trajectory in the phase plane creates a turning point in the physical space, and therefore the corresponding solutions have no physical meaning.

The set of equations (2.38) has three critical points, where $\mathrm{d}f/\mathrm{d}\chi = \mathrm{d}g/\mathrm{d}\chi = 0$. They are $A(0, 0)$, $B\left(1, 2/3\right)$ and $C\left(1/k^2, -2/3k^3\right)$. We shall consider point A first. The linear approximation of (2.38) about this point is written as

$$\frac{\mathrm{d}f}{\mathrm{d}\chi} = 2f + 3(k-1)g, \qquad \frac{\mathrm{d}g}{\mathrm{d}\chi} = 3g, \tag{2.39}$$

with the general solution being

$$f = C_1\mathrm{e}^{2\chi} + C_2\mathrm{e}^{3\chi}, \qquad g = \frac{C_2}{3(k-1)}\,\mathrm{e}^{3\chi}, \tag{2.40}$$

where C_1 and C_2 are arbitrary constants. Elimination of the independent variable χ from (2.40) leads to

$$f - 3(k-1)g = cg^{2/3}, \qquad c = C_1\left[\frac{3(k-1)}{C_2}\right]^{2/3}. \tag{2.41}$$

We see that point A is a node; its two half-lines being

$$g = \frac{1}{3(k-1)}f, \qquad g = 0. \tag{2.42a,b}$$

In order to establish the correspondence between the phase plane (f, g) and the solution behaviour in the physical plane, we must use equation 2.37, which on noting that $f \approx 0$ near A, may be written as

$$\mathrm{d}\chi = -\frac{1}{k}\frac{\mathrm{d}\xi}{\xi}.$$

Performing the integration, we find

$$\chi = \widetilde{C} - \frac{1}{k}\ln|\xi|. \tag{2.43}$$

Let us now return to equations (2.40). They show that point A is reached in the limit when $\chi \to -\infty$. According to (2.43), this is achieved by setting $|\xi| \to \infty$. Hence, point A in the phase plane represents the body surface both upstream and downstream of point O (see figure 4). For the flow upstream of O, the asymptotic formula (2.23) is valid. Recasting this formula in terms of functions f and g through (2.35), (2.36) and eliminating ξ, yields

$$f = cg^{2/3}, \tag{2.44}$$

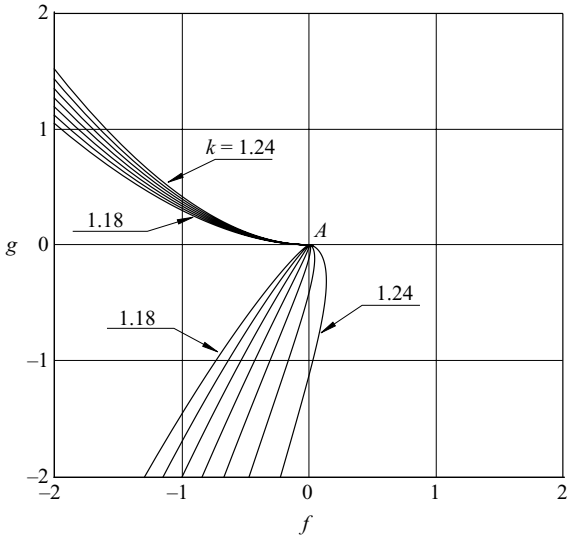

FIGURE 7. Phase plane representation of the solutions shown in figure 5.

where

$$c = -\left(3 - \frac{2}{k}\right)\frac{d_0}{d_1^{2/3}}.$$

Notice that (2.44) represents the leading-order approximation to (2.41) in a neighbourhood of point A where both f and g are small. Notice further that the particular solution for the body surface that is flat upstream of point O should satisfy condition (2.24), in which case $c = \infty$. The corresponding trajectory in the phase plane emanates from the node point A along the half-line (2.42*b*). A more precise equation for the shape of the trajectory,

$$g = (2k - 2)f^2, \tag{2.45}$$

may be deduced by manipulating (2.31) instead of (2.23).

The flow near the body surface downstream of point O is described by the asymptotic expansion (2.25). Using (2.25) in (2.35) and (2.36) also leads to (2.44), now with

$$c = \left(3 - \frac{2}{k}\right)\frac{b_0}{b_1^{2/3}}.$$

Figure 7 is the phase plane representation of the solutions shown in figure 5. As was predicted, all the trajectories emerge from point A at $\xi = -\infty$ and follow the parabola 2.45 along its left-hand side branch. This is a consequence of the assumption that the flow is subsonic ($u < 1$) before the corner which, according to (2.36) and (2.32), requires that $f < 0$. The solution remains in the subsonic half-plane ($f < 0$) for all $\xi < 0$. As $\xi \to 0^-$, the point in the phase plane (f, g) approaches infinity, simply by virtue of the definition (2.36) of functions f and g. Both $F(\xi)$ and $G(\xi)$ in (2.36) remain continuous at $\xi = 0$. Therefore, as ξ crosses over to positive values, function f remains unchanged while g changes its sign. This means that the solution jumps (through the 'infinity') to another trajectory being reflected in the f-axis. As ξ increases further, the solution returns to point A, remaining all the way in the subsonic half-plane provided that $k < 6/5$. When parameter k increases beyond $k = 6/5$, a part of the trajectory crosses

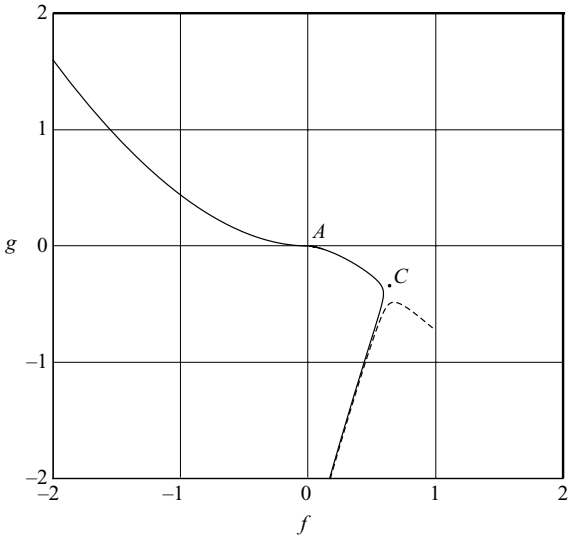

FIGURE 8. The solution behaviour for $k = 1.249$ (solid line) and $k = 1.251$ (dashed line).

over to the right-half plane, signifying that the corresponding region in the flow field appears to be supersonic.

What happens in the vicinity of $k = 1.25$ is illustrated by figure 8. We can see that because of the presence of critical point $C\left(1/k^2, -2/3k^3\right)$, the solution drastically changes its behaviour when parameter k passes through $k = 5/4$. For any $k < 5/4$, no matter how close to $k = 5/4$, the trajectory still returns to point A, but for $k > 5/4$, it turns away toward the singular line $f = 1$. This line is reached at a finite value ξ_s of the self-similar variable ξ, signifying that the corresponding solution cannot represent a real flow.

We shall now examine the behaviour of the solution near critical point $C\left(1/k^2, -2/3k^3\right)$. The linear approximation of equations (2.38) about this point has the form

$$\begin{aligned} \frac{\mathrm{d}f}{\mathrm{d}\chi} &= \frac{2}{k}(k-2)\left(f - \frac{1}{k^2}\right) + 3(k-1)\left(g + \frac{2}{3k^3}\right), \\ \frac{\mathrm{d}g}{\mathrm{d}\chi} &= \frac{2}{k^2}(2k-1)\left(f - \frac{1}{k^2}\right) + \frac{3}{k}(k-1)\left(g + \frac{2}{3k^3}\right). \end{aligned} \tag{2.46}$$

The general solution of (2.46) is written as

$$f - \frac{1}{k^2} = C_1 \exp(\lambda_1 \chi) + C_2 \exp(\lambda_2 \chi),\ g + \frac{2}{3k^3} = -\frac{1}{k} C_1 \exp(\lambda_1 \chi) + \frac{2(2k-1)}{3k(k-1)} C_2 \exp(\lambda_2 \chi), \tag{2.47}$$

where

$$\lambda_1 = -\left(\frac{1}{k} + 1\right), \qquad \lambda_2 = 6\left(1 - \frac{1}{k}\right).$$

Elimination of the independent variable χ from (2.47) leads to

$$\left[\frac{\tilde{g} - \alpha \tilde{f}}{C_2(\beta - \alpha)}\right]^{\lambda_1} = \left[\frac{\tilde{g} - \beta \tilde{f}}{C_1(\alpha - \beta)}\right]^{\lambda_2}, \tag{2.48}$$

where

$$\tilde{f} = f - \frac{1}{k^2}, \quad \tilde{g} = g + \frac{2}{3k^3}, \quad \alpha = -\frac{1}{k}, \quad \beta = \frac{2(2k-1)}{3k(k-1)}.$$

Since λ_1 and λ_2 have opposite signs, equation (2.48) represents a saddle point. Its separatrices are

$$g + \frac{2}{3k^3} = -\frac{1}{k}\left(f - \frac{1}{k^2}\right), \qquad g + \frac{2}{3k^3} = \frac{2(2k-1)}{3k(k-1)}\left(f - \frac{1}{k^2}\right). \tag{2.49a,b}$$

We shall study (2.49*b*) in detail, as it apparently represents the limiting trajectory in the phase plane as $k \to 5/4$ (see figure 8). For the solution to find itself on this separatrix, we have to choose $C_1 = 0$ in (2.47). This yields

$$f = \frac{1}{k^2} + C_2 \exp(\lambda_2 \chi), \qquad g = -\frac{2}{3k^3} + \frac{2(2k-1)}{3k(k-1)} C_2 \exp(\lambda_2 \chi). \tag{2.50}$$

Near point C, equation (2.37) may be written as

$$\mathrm{d}\chi = \frac{\mathrm{d}\xi}{(1/k^2 - 1)\, k\xi}$$

which can be integrated to give

$$\chi = \widetilde{C} - \frac{k}{k^2 - 1} \ln|\xi|. \tag{2.51}$$

Since λ_2 is positive for any $k > 1$, we can conclude from (2.50) that point C is reached when $\chi \to -\infty$. According to (2.51), this is only possible if $|\xi| \to \infty$.

Substitution of (2.51) into (2.50) results in

$$\left.\begin{aligned} f &= \frac{1}{k^2} + \widehat{C}|\xi|^{-6/(k+1)} + \cdots \\ g &= -\frac{2}{3k^3} + \frac{2(2k-1)}{3k(k-1)}\widehat{C}|\xi|^{-6/(k+1)} + \cdots \end{aligned}\right\} \quad \text{as} \quad |\xi| \to \infty, \tag{2.52}$$

where we have put

$$\widehat{C} = C_2 \exp(6\widetilde{C}(1 - 1/k)).$$

2.3. *Transonic Prandtl–Meyer flow*

Here, we aim to demonstrate that the trajectory in the phase plane that terminates at the saddle point C represents transonic flow accelerating into a supersonic Prandtl–Meyer fan. It is well known that a complete description of the Prandtl–Meyer flow field is given by the equation (see, for example, Liepmann & Roshko 1957)

$$\vartheta + \sigma(\lambda) = \text{const.} \tag{2.53}$$

Here, ϑ is the angle made by the velocity vector with the x-axis, λ is the normalized velocity

$$\lambda = \frac{\sqrt{\hat{u}^2 + \hat{v}^2}}{V_0} = \sqrt{u^2 + v^2},$$

and $\sigma(\lambda)$ the Prandtl–Meyer function

$$\sigma(\lambda) = \int_1^{\lambda} \sqrt{\frac{\lambda^2 - 1}{1 - (\gamma - 1)/(\gamma + 1)\lambda^2}}\, \frac{\mathrm{d}\lambda}{\lambda}. \tag{2.54}$$

In the transonic speed range, $\lambda - 1 \ll 1$, and thus we may approximate the integral (2.54) as

$$\sigma(\lambda) = \tfrac{2}{3}\sqrt{\gamma+1}\,(\lambda-1)^{3/2} + \cdots \quad \text{as} \quad \lambda \to 1, \tag{2.55}$$

and it follows from (2.53) that with small $\lambda - 1$, the directional angle ϑ must also be small, namely, $\lambda - 1 = O(\vartheta^{2/3})$. Taking this into account, we can deduce that

$$u = \lambda\cos\vartheta = 1 + (\lambda - 1) + O(\vartheta^2), \qquad v = \lambda\sin\vartheta = \vartheta + O\left(\vartheta^{5/3}\right),$$

which allows us to write (2.55) as $\sigma(\lambda) = \frac{2}{3}\sqrt{\gamma+1}\,(u-1)^{3/2}$, and the Prandtl–Meyer equation (2.53) takes the form

$$v + \tfrac{2}{3}\sqrt{\gamma+1}\,(u-1)^{3/2} = \text{const}. \tag{2.56}$$

Finally, we substitute (2.32) into (2.56). Here, for the solution to be self-similar, the constant on the right-hand side of (2.56) should be set to zero, leading to

$$G + \tfrac{2}{3}F^{3/2} = 0. \tag{2.57}$$

Substitution of (2.35) into (2.57) yields

$$(3k-2)F_0(\xi) - k\xi F_0'(\xi) + \tfrac{2}{3}[F_0'(\xi)]^{2/3} = 0.$$

It is easily verified that the solution of this equation has the form

$$F_0(\xi) = \tfrac{1}{3}\xi^3. \tag{2.58}$$

Substituting (2.58) back into (2.35), and calculating f and g with the help of (2.36), we have

$$f = \frac{1}{k^2}, \qquad g = -\frac{2}{3k^3}.$$

This shows that formula (2.58) represents only the final point of the trajectory we are interested in, namely, the saddle point C. Hence, (2.58) should be treated as the leading-order term of the asymptotic expansion of function $F_0(\xi)$ as $\xi \to \infty$. The next-order term may be determined directly from equation (2.22). We find

$$F_0(\xi) = \tfrac{1}{3}\xi^3 + \breve{a}\,\xi^{3(k-1)/(k+1)} + \cdots \quad \text{as} \quad \xi \to \infty, \tag{2.59}$$

where $\breve{a}$ is a constant. Calculating f and g again, yields

$$\left.\begin{aligned} f &= \frac{1}{k^2} + \frac{3\breve{a}}{k^2}\frac{k-1}{k+1}\xi^{-6/(k+1)} + \cdots \\ g &= -\frac{2}{3k^3} + \frac{2\breve{a}}{k^3}\frac{2k-1}{k+1}\xi^{-6/(k+1)} + \cdots \end{aligned}\right\} \quad \text{as} \quad \xi \to \infty. \tag{2.60}$$

Comparison of (2.60) with (2.52) shows that (2.59) indeed represents the solution that approaches the saddle point C along the separatrix (2.49*b*). It further follows from (2.60) that for the saddle point to be approached from below, as figure 8 suggests, constant $\breve{a}$ in (2.60) should be negative.

We now return to the task of calculating the solution of equation (2.22) for $k = 5/4$. In order to avoid the problem with 'branching' of the solution on the approach to the critical point C (see figure 8), the integrations can be performed backwards starting from a large enough positive value of ξ, where the initial conditions for function F_0 and its derivative F_0' can be prescribed using (2.59). Constant $\breve{a}$ in (2.59) can be set to $\breve{a} = -1$ without loss of generality thanks to the invariant transformation (2.30). The results of the calculations are shown in figure 9, where F_0' is plotted against ξ.

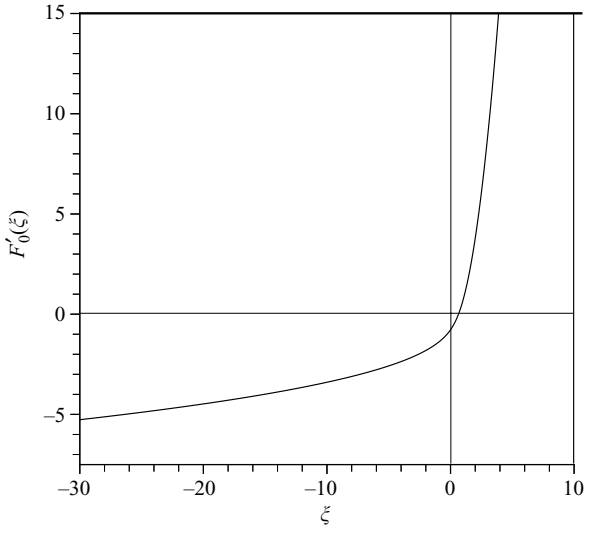

FIGURE 9. Results of the numerical solution of equation (2.22) for $k = 5/4$.

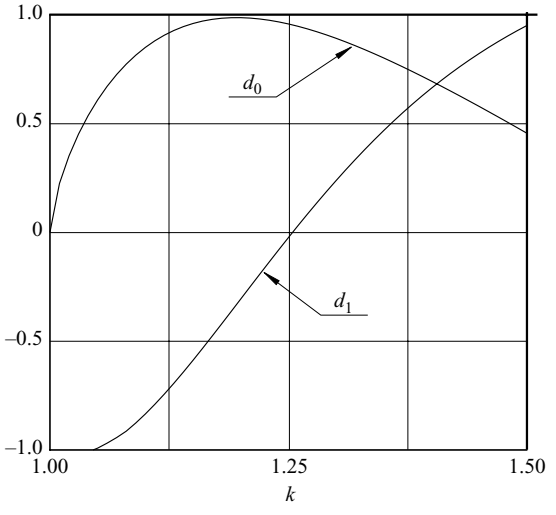

FIGURE 10. The behaviour of the coefficients d_0 and d_1 of the asymptotic expansion (2.23).

Of course, this sort of calculation, when equation (2.22) is solved with downstream boundary condition (2.59), may be conducted for other values of k. The coefficients d_0 and d_1 of the asymptotic expansion (2.23) may be easily extracted from the numerical solution, and their behaviour is shown in figure 10. We see that the impermeability condition (2.24) is satisfied only for one value of k, namely, for $k = 5/4$.

The possibility of the solution described above existing was earlier seen by Guderley (1948). His analysis was based on the hodograph method, which allowed him to construct the solution in an analytical form. However, at the time, the physical meaning of the hodograph solution was unclear. Now the analysis presented above shows that the solution corresponds to a Prandtl–Meyer fan. The exact form of the solution is of little relevance for the analysis in the rest paper, and it suffices to note that Guderley's solution confirms that parameter k is not just close to 1.25, as the

numerical solution suggests, but equals precisely 5/4. For a discussion of various aspects of this type of flow, see also Vaglio-Laurin (1960) and Diyesperov (1994).

2.4. *Physical interpretation of the results*

The above analysis shows that in transonic flow over a rigid body whose surface has the form defined by (2.14), two flow regimes can be distinguished. Provided $1 < k < 5/4$ (which corresponds to $1 < \alpha < 8/5$) the solution is uniquely defined by the body shape. In particular, parameter k is given by (2.28), and coefficient b_1 in the downstream asymptotic expansion (2.25) is related to factor a in (2.14) through equation (2.29). For $k \in (1, 6/5)$ the flow remains subsonic everywhere, and it is natural that the flow depends on the boundary conditions both upstream and downstream of point O. We found that for $6/5 < k < 5/4$, a supersonic region forms in the flow downstream of point O. Despite this, the solution remains dependent on the body shape behind point O, which means that the perturbations are still capable of propagating through the flow in the upstream direction. This is because the characteristics originating from the surface downstream intersect with the sonic line, and thus the disturbances (including the influence of the downstream boundary) can reach the sonic line first, after which they propagate upstream in the subsonic region of the flow.

However, as soon as parameter k reaches its critical value $k = 5/4$, the flow exhibits very fast acceleration into the Prandtl–Meyer fan (see figure 9) which 'blocks' upstream propagation of the perturbations. As a result the flow field 'freezes', in the sense that it can no longer change with further bending of the body contour downstream of point O. This suggests that the solution with $k = 5/4$ is actually applicable to a variety of flows, where the gas undergoes acceleration from subsonic to supersonic speed to form a Prandtl–Meyer fan around a corner (or, more generally, a point where the body curvature is discontinuous). The supersonic flow shown in figure 3 obviously belongs to this category.

Before turning to the flow analysis in the boundary layer, we must calculate the pressure acting upon the boundary layer on the approach to point O (see figure 4). Substituting (2.23) into (2.21) and recalling that $\xi = x/y^k$, we find

$$p = \frac{d_0}{\gamma + 1}\left(3 - \frac{2}{k}\right)(-x)^{2-2/k} + \cdots \quad \text{as} \quad x \to 0^-.$$

For the limiting case $k = 5/4$, which will be the focus of the rest of the paper, we have,

$$p\Big|_{y=0} = \kappa(-x)^{2/5} + \cdots \quad \text{as} \quad x \to 0^-, \tag{2.61}$$

where

$$\kappa = \frac{7}{5}\frac{d_0}{\gamma + 1}.$$

3. Classical boundary layer upstream of the interaction region

For the analysis of the flow in the boundary layer that forms on the body surface, it is convenient to use orthogonal curvilinear coordinates $\hat{x}'$, $\hat{y}'$ where $\hat{x}'$ is measured along the body contour from point O and $\hat{y}'$ in the perpendicular direction (11). The velocity components in these coordinates will be denoted by $\hat{u}'$ and $\hat{v}'$. The pressure and gas density are denoted, as before, by $\hat{p}$ and $\hat{\rho}$. In the boundary layer, we must also consider the enthalpy $\hat{h}$ and dynamic viscosity $\hat{\mu}$. The non-dimensional variables

are similar to (2.7),

$$\hat{u}' = \hat{V}_0 u', \quad \hat{v}' = \hat{V}_0 v', \quad \hat{p} = \hat{p}_0 + \hat{\rho}_0 \hat{V}_0^2 p,$$
$$\hat{\rho} = \hat{\rho}_0 \rho, \quad \hat{h} = \hat{V}_0^2 h, \quad \hat{\mu} = \hat{\mu}_0 \mu,$$
$$\hat{x} = Lx', \quad \hat{y} = Ly'.$$

Recall that suffix '0' indicates the values of the corresponding quantities immediately outside the boundary layer at point O of the body contour, where the gas velocity coincides with the speed of sound.

In what follows, we shall assume that the Reynolds number,

$$Re = \frac{\hat{\rho}_0 \hat{V}_0 L}{\hat{\mu}_0},$$

is large. The asymptotic expansions of the gas dynamic functions in the boundary layer (in what follows we shall call it region 2) are sought in the form

$$\left.\begin{array}{ll} u'(x', y'; Re) = U_0(x', Y) + \cdots, & v'(x', y'; Re) = Re^{-1/2} V_0(x', Y) + \cdots, \\ p(x', y'; Re) = P_0(x', Y) + \cdots, & \rho(x', y'; Re) = R_0(x', Y) + \cdots, \\ h(x', y'; Re) = h_0(x', Y) + \cdots, & \mu(x', y'; Re) = \mu_0(x', Y) + \cdots, \end{array}\right\} \tag{3.1}$$

where, as usual, the coordinate normal to the wall is scaled as

$$Y = Re^{1/2} y'.$$

Substitution of (3.1) into the Navier–Stokes equations yields

$$R_0\left(U_0 \frac{\partial U_0}{\partial x'} + V_0 \frac{\partial U_0}{\partial Y}\right) = -\frac{\partial P_0}{\partial x'} + \frac{\partial}{\partial Y}\left(\mu_0 \frac{\partial U_0}{\partial Y}\right), \tag{3.2}$$

$$R_0\left(U_0 \frac{\partial h_0}{\partial x'} + V_0 \frac{\partial h_0}{\partial Y}\right) = U_0 \frac{\partial P_0}{\partial x'} + \frac{1}{Pr} \frac{\partial}{\partial Y}\left(\mu_0 \frac{\partial h_0}{\partial Y}\right) + \mu_0 \left(\frac{\partial U_0}{\partial Y}\right)^2, \tag{3.3}$$

$$\frac{\partial (R_0 U_0)}{\partial x'} + \frac{\partial (R_0 V_0)}{\partial Y} = 0, \tag{3.4}$$

$$h_0 = \frac{1}{(\gamma - 1) R_0} + \frac{\gamma}{\gamma - 1} \frac{P_0}{R_0}. \tag{3.5}$$

Equations (3.2)–(3.5) are, respectively, the momentum equation projected upon the longitudinal coordinate x', the energy equation with Pr being the Prandtl number, the continuity equation and the state equation. It further follows from the y'-component of the momentum equation that

$$\frac{\partial P_0}{\partial Y} = 0,$$

i.e. to the leading-order approximation, the pressure does not change across the boundary layer. Hence, using (2.61), we can conclude that inside the boundary layer

$$\frac{\partial P_0}{\partial x'} = -\tfrac{2}{5} \kappa (-x')^{-3/5} + \cdots \quad \text{as} \quad x' \to 0^-. \tag{3.6}$$

Here it is noted that to the left of point O, where the body surface is flat, the Cartesian coordinates, (x, y), coincide with curvilinear coordinates, (x', y').

We shall now construct asymptotic solution of equations (3.2)–(3.5) as $x' \to 0^-$. Since the boundary layer is exposed to the singular pressure gradient (3.6), it splits up into two subregions, the main part of the boundary layer shown in figure 11 as region 2*a* and near-wall sublayer 2*b*. We shall start with the sublayer 2*b*.

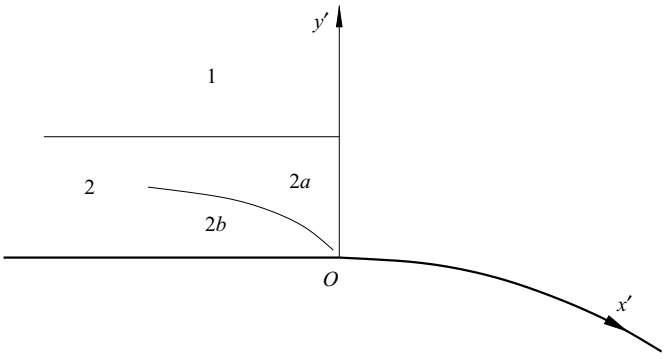

FIGURE 11. Splitting of the boundary layer upstream of the interaction region.

3.1. *Region 2b*

Taking into account that the fluid particles in region 2*b* experience extreme acceleration caused by the singular favourable pressure gradient, we have to expect that the convective terms on the left-hand side of the momentum equation (3.2) are of the same order of magnitude as the pressure gradient on the right-hand side of this equation, which may be expressed as follows

$$R_0 U_0 \frac{\partial U_0}{\partial x'} \sim \frac{\partial P_0}{\partial x'}. \tag{3.7}$$

Since the no-slip condition at the aerofoil surface has to be satisfied by the solution in region 2*b*, we further require that the flow in this region be viscous, i.e.

$$R_0 U_0 \frac{\partial U_0}{\partial x'} \sim \frac{\partial}{\partial Y}\left(\mu_0 \frac{\partial U_0}{\partial Y}\right). \tag{3.8}$$

Let us denote the value of the non-dimensional enthalpy h_0 at the 'bottom' of the boundary layer at point O by h_w. The corresponding values of the non-dimensional density R_0 and viscosity μ_0 will be denoted by ρ_w and μ_w, respectively. If the body surface is not artificially heated or cooled, then ρ_w and μ_w are order-one quantities. Taking this into account, we can deduce from (3.7) and (3.6) that in the viscous sublayer 2*b*

$$U_0 \sim (-x')^{1/5}. \tag{3.9}$$

Using (3.9) in (3.8), we find that the thickness of region 2*b* is estimated as

$$Y \sim (-x')^{2/5}. \tag{3.10}$$

Since the flow is two-dimensional, it is convenient to use the stream function $\Psi_0(x', Y)$. Its existence follows from the continuity equation (3.4), which shows that this function should be defined such that

$$\frac{\partial \Psi_0}{\partial Y} = R_0 U_0, \qquad \frac{\partial \Psi_0}{\partial x'} = -R_0 V_0. \tag{3.11a,b}$$

From (3.11*a*) and estimates (3.9) and (3.10) it follows that

$$\Psi_0 \sim U_0 Y \sim (-x')^{3/5}.$$

This suggests that the asymptotic expansion of the stream function in the viscous sublayer 2*b* should be sought in the form

$$\Psi_0(x', Y) = (-x')^{3/5}\psi(\eta) + \cdots \quad \text{as} \quad x' \to 0^-, \tag{3.12}$$

where, on account of (3.10), the similarity variable η is defined as

$$\eta = \frac{Y}{(-x')^{2/5}}. \tag{3.13}$$

In order to deduce the form of the asymptotic expansions of the density R_0 and dynamic viscosity μ_0, one needs to estimate the enthalpy variations in region 2*b* by using the energy equation (3.3). Comparing the heat transfer term on the right-hand side of this equation with the mechanical energy dissipation

$$\frac{1}{Pr}\frac{\partial}{\partial Y}\left(\mu_0 \frac{\partial h_0}{\partial Y}\right) \sim \mu_0 \left(\frac{\partial U_0}{\partial Y}\right)^2,$$

we see that the variations of the enthalpy

$$|h_0 - h_w| \sim U_0^2 \sim (-x')^{2/5}.$$

Using further the state equation (3.5) we have

$$|R_0 - \rho_w| \sim (-x')^{2/5},$$

and, since the viscosity μ_0 is a function of the enthalpy, we can write

$$|\mu_0 - \mu_w| \sim (-x')^{2/5}.$$

This shows that the sought asymptotic expansions of the density and viscosity in region 2*b* may be represented in the form

$$\left.\begin{aligned} R_0(x', Y) &= \rho_w + (-x')^{2/5}\tilde{\rho}(\eta) + \cdots \\ \mu_0(x', Y) &= \mu_w + (-x')^{2/5}\tilde{\mu}(\eta) + \cdots \end{aligned}\right\} \quad \text{as} \quad x' \to 0^-. \tag{3.14a,b}$$

In the viscous sublayer, it suffices to know the leading terms, so the solution for the correction terms, $\tilde{\rho}$ and $\tilde{\mu}(\eta)$, need not be worked out.

Substitution of (3.12) and (3.13) together with (3.14) into (3.11) and then into (3.2) results in the following equation for $\psi(\eta)$:

$$\mu_w \psi''' - \tfrac{3}{5}\psi\psi'' + \tfrac{1}{5}(\psi')^2 + \tfrac{2}{5}\kappa\rho_w = 0. \tag{3.15}$$

It should be solved subject to the no-slip condition on the rigid-body surface

$$\psi(0) = \psi'(0) = 0, \tag{3.16}$$

and a requirement that $\psi(\eta)$ does not grow exponentially as $\eta \to \infty$; an exponentially growing $\psi(\eta)$ must be ruled out because otherwise the matching of solutions in regions 2*b* and 2*a* (see figure 11) would be impossible.

The latter suggests that the leading-order term of the asymptotic expansion of function $\psi(\eta)$ near the outer edge of the viscous sublayer should be sought in the algebraic form

$$\psi(\eta) = A\eta^\alpha + \cdots \quad \text{as} \quad \eta \to \infty, \tag{3.17}$$

where A and α are unknown constants. Differentiating (3.17), we find

$$\begin{aligned} \mu_w \psi''' &= \mu_w A\alpha(\alpha-1)(\alpha-2)\eta^{\alpha-3} + \cdots, \\ \tfrac{3}{5}\psi\psi'' &= \tfrac{3}{5}A^2\alpha(\alpha-1)\eta^{2\alpha-2} + \cdots, \\ \tfrac{1}{5}(\psi')^2 &= \tfrac{1}{5}A^2\alpha^2\eta^{2\alpha-2} + \cdots. \end{aligned}$$

This shows that, if we assume (subject to subsequent confirmation) that $\alpha > 1$, then the first and fourth terms in equation (3.15), representing the viscous force and pressure

gradient, respectively, appear to be small as compared to the second and third terms, and therefore, at large η, equation (3.15) reduces to

$$\tfrac{1}{5}A^2[\alpha^2 - 3\alpha(\alpha-1)]\eta^{2\alpha-2} = 0.$$

Since we are looking for a non-trivial solution ($A \neq 0$), we have to set $\alpha^2 - 3\alpha(\alpha-1) = 0$. This quadratic has two roots

$$\alpha = \tfrac{3}{2}, \qquad \alpha = 0.$$

Only the first of these satisfies condition $\alpha > 1$, and we can conclude that the leading-order term (3.17) of the asymptotic expansion of function $\psi(\eta)$ is written as

$$\psi(\eta) = A\eta^{3/2} + \cdots \quad \text{as} \quad \eta \to \infty.$$

Let us now find the next-order term. We write

$$\psi(\eta) = A\eta^{3/2} + B\eta^{\beta} + \cdots \quad \text{as} \quad \eta \to \infty, \tag{3.18}$$

where B is a constant. Since the second term in (3.18) has to be small compared to the first one, we have to assume that

$$\beta < \tfrac{3}{2}. \tag{3.19}$$

Differentiating (3.18), we find

$$\mu_w\psi''' = -\tfrac{3}{8}A\mu_w\eta^{-3/2} + \mu_w B\beta(\beta-1)(\beta-2)\eta^{\beta-3} + \cdots,$$

$$\tfrac{3}{5}\psi\psi'' = \tfrac{9}{20}A^2\eta + \tfrac{3}{5}AB\left[\tfrac{3}{4} + \beta(\beta-1)\right]\eta^{\beta-1/2} + \cdots, \tag{3.20}$$

$$\tfrac{1}{5}(\psi')^2 = \tfrac{9}{20}A^2\eta + \tfrac{3}{5}AB\beta\eta^{\beta-1/2} + \cdots. \tag{3.21}$$

Obviously, the viscous term is negligible compared with the two inertia terms. If $\beta > 1/2$, the pressure gradient $2\kappa\rho_w/5$ is negligible in equation (3.15), which then reduces to

$$AB\left(\beta^2 - 2\beta + \tfrac{3}{4}\right)\eta^{\beta-1/2} = 0.$$

It follows that $\beta^2 - 2\beta + 3/4 = 0$. The two roots of this equation are

$$\beta = \tfrac{3}{2}, \qquad \beta = \tfrac{1}{2}.$$

The first one does not satisfy restriction (3.19), and therefore should be disregarded. However, if we choose the second root, $\beta = 1/2$, then the pressure gradient $2\kappa\rho_w/5$ in (3.15) interferes with the balance of the inertial (i.e. the second terms in (3.20) and (3.21)) terms since they are all of the same order. A dilemma then arises because the inertial terms cancel out, leaving nothing to balance the pressure. Situations like this are normally resolved by introducing logarithmic terms. We shall use, instead of (3.18), the following asymptotic expansion

$$\psi(\eta) = A\eta^{3/2} + \tilde{B}\eta^{1/2}\ln\eta + B\eta^{1/2} + \cdots \quad \text{as} \quad \eta \to \infty. \tag{3.22}$$

Substitution of (3.22) into equation (3.15) yields

$$\tilde{B} = -\frac{2}{3}\frac{\kappa\rho_w}{A},$$

where A, $\tilde{B}$ and B are constants. They are determined by solving the boundary-value problem (3.15)–(3.16). The parameters in (3.15) can be eliminated by suitably rescaling both the dependent and independent variables. Using the numerical solution of the

resulting canonical equation, we find that

$$A \approx 1.38\mu_w(\kappa\rho_w/\mu_w^2)^{5/8}, \qquad \tilde{B} \approx -0.48\mu_w(\kappa\rho_w/\mu_w^2)^{3/8},$$
$$B \approx \mu_w(\kappa\rho_w/\mu_w^2)^{3/8}\big(-1.61 - 0.48\ln(\kappa\rho_w/\mu_w^2)^{1/4}\big).$$

In order to determine the velocity components in region 2*b*, we must substitute (3.12), (3.13) and (3.14*a*) into equations (3.11). This results in

$$\left.\begin{aligned} U_0 &= (-x')^{1/5}\frac{1}{\rho_w}\psi'(\eta) + \cdots \\ V_0 &= (-x')^{-2/5}\frac{1}{\rho_w}\left(\frac{3}{5}\psi - \frac{2}{5}\eta\psi'\right) + \cdots \end{aligned}\right\} \quad \text{as} \quad x' \to 0^-. \tag{3.23}$$

Substituting (3.22) into (3.23), we find that at the outer edge of region 2*b*

$$\left.\begin{aligned} U_0 &= (-x')^{1/5}\frac{1}{\rho_w}\left[\tfrac{3}{2}A\eta^{1/2} + \tfrac{1}{2}\tilde{B}\eta^{-1/2}\ln\eta + \big(\tilde{B} + \tfrac{1}{2}B\big)\eta^{-1/2}\right] + \cdots, \\ V_0 &= (-x')^{-2/5}\frac{1}{\rho_w}\left[\tfrac{2}{5}\tilde{B}\eta^{1/2}\ln\eta + \tfrac{2}{5}(B - \tilde{B})\eta^{1/2}\right] + \cdots. \end{aligned}\right\} \tag{3.24}$$

3.2. *Region 2a*

Asymptotic analysis of the boundary-layer equations (3.2)–(3.5) in the main part of the boundary layer (region 2*a* in figure 11) is based on the limit procedure

$$Y = O(1), \qquad x' \to 0^-.$$

The form of the solution in this region may be deduced based on the matching principle of asymptotic expansions. According to Kaplun's extension theorem, formulae (3.24) are valid in the overlapping region situated between the viscous sublayer 2*b* and the main part of the boundary layer 2*a*. Therefore, they may also be used at the 'bottom' of region 2*a*. Rewriting (3.24) in terms of Y using (3.13), we have

$$U_0 = \frac{3A}{2\rho_w}Y^{1/2} + (-x')^{2/5}\ln(-x')\left\{-\frac{\tilde{B}}{5\rho_w}\frac{1}{Y^{1/2}}\right\} + (-x')^{2/5}\left\{\frac{\tilde{B}}{2\rho_w}\frac{\ln Y}{Y^{1/2}} + \left(\frac{\tilde{B}}{\rho_w} + \frac{B}{2\rho_w}\right)\frac{1}{Y^{1/2}}\right\} + \cdots, \tag{3.25}$$

$$V_0 = (-x')^{-3/5}\ln(-x')\left\{-\frac{4\tilde{B}}{25\rho_w}Y^{1/2}\right\} + (-x')^{-3/5}\left\{\frac{2\tilde{B}}{5\rho_w}Y^{1/2}\ln Y + \frac{2}{5}\frac{B - \tilde{B}}{\rho_w}Y^{1/2}\right\} + \cdots. \tag{3.26}$$

Guided by (3.25) and (3.26) as well as the matching principle, we represent the solution in region 2*a* in the form of the coordinate expansions

$$\left.\begin{aligned} U_0(x', Y) &= U_{00}(Y) + (-x')^{2/5}\ln(-x')U_{01}(Y) + (-x')^{2/5}U_{02}(Y) + \cdots, \\ V_0(x', Y) &= (-x')^{-3/5}\ln(-x')V_{01}(Y) + (-x')^{-3/5}V_{02}(Y) + \cdots, \\ R_0(x', Y) &= R_{00}(Y) + (-x')^{2/5}\ln(-x')R_{01}(Y) + (-x')^{2/5}R_{02}(Y) + \cdots, \\ h_0(x', Y) &= h_{00}(Y) + (-x')^{2/5}\ln(-x')h_{01}(Y) + (-x')^{2/5}h_{02}(Y) + \cdots, \\ \mu_0(x', Y) &= \mu_{00}(Y) + O\big[(-x')^{2/5}\ln(-x')\big], \end{aligned}\right\} \tag{3.27}$$

valid as $x' \to 0^-$ and $Y = O(1)$. It further follows from (3.25) and (3.26) that the conditions of matching with the solution in region 2*b* are

$$\left.\begin{aligned} U_{00}(Y) &= \frac{3A}{2\rho_w} Y^{1/2} + \cdots \\ V_{01}(Y) &= -\frac{4\tilde{B}}{25\rho_w} Y^{1/2} + \cdots \\ V_{02}(Y) &= \frac{2\tilde{B}}{5\rho_w} Y^{1/2} \ln Y + \frac{2B - 2\tilde{B}}{5\rho_w} Y^{1/2} + \cdots \end{aligned}\right\} \quad \text{as} \quad Y \to 0. \qquad (3.28a\text{–}c)$$

We now substitute (3.27) into the boundary-layer equations (3.2)–(3.5). In the leading-order approximation we have

$$-\tfrac{2}{5} U_{00} U_{01} + U'_{00} V_{01} = 0, \qquad (3.29a)$$

$$-\tfrac{2}{5} U_{00} h_{01} + h'_{00} V_{01} = 0, \qquad (3.29b)$$

$$-\tfrac{2}{5} R_{00} U_{01} - \tfrac{2}{5} U_{00} R_{01} + (R_{00} V_{01})' = 0, \qquad (3.29c)$$

$$h_{00} = \frac{1}{\gamma - 1} \frac{1}{R_{00}}, \qquad h_{01} = -\frac{1}{\gamma - 1} \frac{R_{01}}{R_{00}^2}. \qquad (3.29d)$$

The next-order equations are

$$-\tfrac{2}{5} U_{00} U_{02} + U'_{00} V_{02} = \tfrac{2}{5} \frac{\kappa}{R_{00}} + U_{00} U_{01}, \qquad (3.30a)$$

$$-\tfrac{2}{5} U_{00} h_{02} + h'_{00} V_{02} = -\tfrac{2}{5} \kappa \frac{U_{00}}{R_{00}} + U_{00} h_{01}, \qquad (3.30b)$$

$$-\tfrac{2}{5} R_{00} U_{02} - \tfrac{2}{5} U_{00} R_{02} + (R_{00} V_{02})' = R_{00} U_{01} + U_{00} R_{01}, \qquad (3.30c)$$

$$h_{02} = -\frac{1}{\gamma - 1} \frac{R_{02}}{R_{00}^2} + \frac{\gamma}{\gamma - 1} \frac{\kappa}{R_{00}}. \qquad (3.30d)$$

We solve the leading-order problem (3.29) first. Substitution of (3.29*d*) into the energy equation (3.29*b*) yields

$$\tfrac{2}{5} U_{00} R_{01} - V_{01} R'_{00} = 0. \qquad (3.31)$$

This equation may be used to eliminate R_{01} from (3.29), leading to

$$\tfrac{2}{5} U_{01} - V'_{01} = 0. \qquad (3.32)$$

Now using (3.32) to eliminate U_{01} from the momentum equation (3.29*a*), we find

$$U_{00} V'_{01} - U'_{00} V_{01} = 0,$$

or, equivalently $(V_{01}/U_{00})' = 0$, which implies that V_{01}/U_{00} does not depend on Y. It follows from the matching conditions (3.28) that

$$V_{01} = -\frac{8\tilde{B}}{75A} U_{00}(Y). \qquad (3.33)$$

Working backwards through equations (3.32), (3.31) and (3.29*d*), we can further find that

$$U_{01} = -\frac{4\tilde{B}}{15A} U'_{00}(Y), \qquad R_{01} = -\frac{4\tilde{B}}{15A} R'_{00}(Y), \qquad h_{01} = -\frac{4\tilde{B}}{15A} h'_{00}(Y).$$

The equations for the second-order problem (3.30) may be manipulated in a similar way. As a result we find, in particular, that

$$\left(\frac{V_{02}}{U_{00}}\right)' = \tfrac{2}{5}\kappa\left(1 - \frac{1}{R_{00}U_{00}^2}\right). \tag{3.34}$$

Since $R_{00}(Y) \to \rho_w$ as $Y \to 0$, it follows from (3.28) that

$$R_{00}U_{00}^2 = \frac{9A^2}{4\rho_w}Y + \cdots \quad \text{as} \quad Y \to 0.$$

Integrating explicitly the singular part of (3.34), we see that the solution satisfying the matching condition is

$$\frac{V_{02}}{U_{00}} = \frac{4}{15}\frac{B-\tilde{B}}{A} - \frac{8}{45}\frac{\kappa\rho_w}{A^2}\ln Y + \tfrac{2}{5}\kappa\int_0^Y \left(1 - \frac{1}{M_{00}^2} + \frac{4\rho_w}{9A^2}\frac{1}{Y}\right)\mathrm{d}Y.$$

Here, function $M_{00}(Y) = U_{00}\sqrt{R_{00}}$ represents the distribution of the Mach number across the boundary layer immediately upstream of the interaction region; the latter will be considered in the next section.

4. The interaction region

The displacement effect of the boundary layer may be described in terms of the angle ϑ made by the streamlines with respect to the body contour. It follows from (3.1), (3.27) and (3.33) that in the main part of the boundary layer (region 2*a*)

$$\begin{aligned}\vartheta = \frac{v'}{u'} = Re^{-1/2}\frac{V_0}{U_0} + \cdots &= Re^{-1/2}(-x')^{-3/5}\ln(-x')\frac{V_{01}}{U_{00}} + \cdots \\ &= Re^{-1/2}(-x')^{-3/5}\ln(-x')\left(-\frac{8\tilde{B}}{75A}\right) + \cdots. \end{aligned} \tag{4.1}$$

Now we can estimate the pressure perturbations p' induced by the displacement effect of the boundary layer. According to the transonic inviscid flow theory, with $\vartheta = O(\delta)$ the pressure perturbations may be estimated as $p \sim \delta^{2/3}$. Therefore, using (4.1), we can write

$$p' \sim \vartheta^{2/3} \sim Re^{-1/3}(-x')^{-2/5}[\ln(-x')]^{2/3}.$$

We see that the pressure induced by the displacement effect experiences unbounded growth as $x \to 0^-$, and despite the small factor $Re^{-1/3}$ it may become the same order as the original pressure (2.61) exerted upon the boundary layer. This happens when

$$(-x')^{2/5} \sim Re^{-1/3}(-x')^{-2/5}\left|\ln(-x')\right|^{2/3}. \tag{4.2}$$

Suppose that $-x' \sim \sigma$. Then it follows that

$$\sigma\left|\ln\sigma\right|^{-5/6} = Re^{-5/12}.$$

This transcendental equation serves to determine σ, the longitudinal extent of the interaction region. In this region, the pressure acting upon the boundary layer can no longer be treated as independent of the flow inside the boundary layer. The interaction region has the usual three-tiered structure sketched in figure 12. It is composed of the viscous sublayer (shown as region 5), the main part of the boundary layer (region 4) and an inviscid potential flow (region 3) situated outside the boundary layer. The

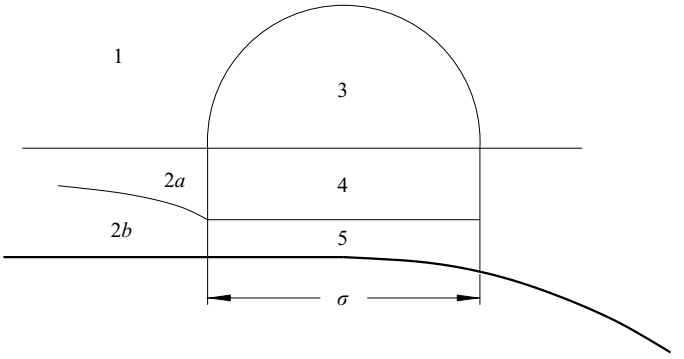

FIGURE 12. A sketch of the interaction region.

lower tier represents a continuation of viscous region $2b$ into the $O(\sigma)$ vicinity of point O (see figure 4).

The middle tier, region 4, is a continuation of region $2a$, and therefore, its thickness is of $O(Re^{-1/2})$. Since the flow in region $2a$ becomes predominantly inviscid as it approaches the interaction region, we can expect the flow in region 4 also to be inviscid. Finally, the upper tier is situated in the potential flow outside the boundary layer. It serves to generate the pressure perturbations in response to the displacement effect of the boundary layer. Also shown in figure 12 is the inviscid region 1 that was studied in detail in § 2.

4.1. *Region* 5

Since η, as defined by (3.13), should remain $O(1)$ in the viscous sublayer $2b$, it follows that the thickness of region 5 may be estimated as

$$y' = Re^{-1/2}Y \sim Re^{-1/2}(-x')^{2/5} \sim Re^{-1/2}\sigma^{2/5}.$$

This means that the asymptotic analysis of the Navier–Stokes equations in region 5 should be based on the limit procedure

$$x_* = \frac{x'}{\sigma(Re)} = O(1), \qquad Y_* = \frac{y' Re^{1/2}}{[\sigma(Re)]^{2/5}} = O(1), \qquad Re \to \infty. \tag{4.3}$$

The form of the asymptotic expansions for the velocity components u', v', pressure p, density ρ and viscosity μ may be inferred by re-expansion of the solution (3.23), (3.14), (2.61) in region $2b$ in terms of variables (4.3). We have

$$\left.\begin{aligned} u'(x', y'; Re) &= \sigma^{1/5} U^*(x_*, Y_*) + \cdots, \\ v'(x', y'; Re) &= Re^{-1/2}\sigma^{-2/5} V^*(x_*, Y_*) + \cdots, \\ p(x', y'; Re) &= \sigma^{2/5} P^*(x_*, Y_*) + \cdots, \\ \rho(x', y'; Re) &= \rho_w + \cdots, \quad \mu(x', y'; Re) = \mu_w + \cdots. \end{aligned}\right\} \tag{4.4}$$

The re-expansion also shows that the matching with the longitudinal velocity component (3.23) in region $2b$ requires that

$$U^*(x_*, Y_*) = (-x_*)^{1/5} \frac{1}{\rho_w} \psi'(\eta) + \cdots \quad \text{as} \quad x_* \to -\infty. \tag{4.5}$$

The argument (3.13) of function $\psi(\eta)$ is expressed in terms of variables (4.3) as

$$\eta = \frac{Y_*}{(-x_*)^{2/5}}. \tag{4.6}$$

Substitution of (4.4) into the Navier–Stokes equations leads to the (incompressible) boundary-layer equations

$$\left.\begin{aligned} &U^*\frac{\partial U^*}{\partial x_*}+V^*\frac{\partial U^*}{\partial Y_*}=-\frac{1}{\rho_w}\frac{\partial P^*}{\partial x_*}+\frac{\mu_w}{\rho_w}\frac{\partial^2 U^*}{\partial Y_*^2},\\ &\frac{\partial P^*}{\partial Y_*}=0,\\ &\frac{\partial U^*}{\partial x_*}+\frac{\partial V^*}{\partial Y_*}=0. \end{aligned}\right\} \tag{4.7}$$

They should be solved with the no-slip conditions on the body surface

$$U^*=V^*=0 \quad \text{at} \quad Y_*=0, \tag{4.8}$$

and initial condition (4.5). Equations (4.7) also require a boundary condition for U^* at the outer edge of region 5. It may be derived as follows. We note that in the main part of the boundary layer (region 4), the longitudinal velocity profile remains unchanged to the leading order. Indeed, the pressure variations in the interaction region are small. According to (4.5), $\Delta p \sim \sigma^{2/5}$. This means that the variations of the longitudinal velocity $\Delta u \sim \sigma^{2/5}$. Hence, in region 4,

$$u(x, y; Re) = U_{00}(Y) + \cdots. \tag{4.9}$$

To perform the matching, we note that in region 4, $y = Re^{-1/2}Y$. On the other hand, in region 5, $y = Re^{-1/2}\sigma^{2/5}Y_*$. Consequently,

$$Y = \sigma^{2/5}Y_*, \tag{4.10}$$

which means that the argument Y of function $U_{00}(Y)$ on the right-hand side of (4.9) is small, and therefore, the (3.28a) is applicable. We have

$$u(x, y; Re) = \sigma^{1/5}\frac{3A}{2\rho_w}Y_*^{1/2} + \cdots. \tag{4.11}$$

Comparing (4.11) with the asymptotic expansion for $u(x, y; Re)$ in (4.4), we find that the sought boundary condition is,

$$U^*(x_*, Y_*) = \frac{3A}{2\rho_w}Y_*^{1/2} + \cdots \quad \text{as} \quad Y_* \to \infty. \tag{4.12}$$

Let us now find the next-order term in (4.12). For this purpose, it is convenient to introduce the stream function $\psi^*(x_*, Y_*)$ such that

$$\frac{\partial \psi^*}{\partial Y_*} = \rho_w U^*, \qquad \frac{\partial \psi^*}{\partial x_*} = -\rho_w V^*. \tag{4.13a,b}$$

Integrating (4.13a) with (4.12), we find

$$\psi^*(x_*, Y_*) = AY_*^{3/2} + \cdots \quad \text{as} \quad Y_* \to \infty.$$

Including the next-order term, we write

$$\psi^*(x_*, Y_*) = AY_*^{3/2} + G(x_*)Y_*^{\alpha} + \cdots \quad \text{as} \quad Y_* \to \infty, \tag{4.14}$$

where it is assumed that $\alpha < 3/2$, and $G(x_*)$ is an arbitrary function. If $\alpha > 1/2$, the convective terms of the left-hand side of momentum equation (4.7) would be larger than the pressure gradient; but the momentum equation then reduces to

$$\left(\alpha - \tfrac{1}{2}\right)G'(x_*) = 0,$$

i.e. a non-trivial solution exists only if $\alpha = 1/2$, for which the pressure gradient actually interferes with the second term $G(x_*)Y_*^{\alpha}$ in (4.14). This suggests that (4.14) should be modified to

$$\psi^*(x_*, Y_*) = AY_*^{3/2} + F(x_*)\,Y_*^{1/2}\ln Y_* + G(x_*)\,Y_*^{1/2} + \cdots \quad \text{as} \quad Y_* \to \infty. \tag{4.15}$$

Substitution of (4.15) into (4.13) and then into the momentum equation (4.7) yields

$$\frac{3A}{2\rho_w}F'(x_*) = -\frac{\mathrm{d}P^*}{\mathrm{d}x_*}. \tag{4.16}$$

The appropriate initial condition for equation (4.16) may be deduced from (4.5). At the outer edge of the viscous sublayer, function $\psi(\eta)$ is given by (3.22) which, being substituted into (4.5), yields

$$U^* = \frac{(-x_*)^{1/5}}{\rho_w}\left[\tfrac{3}{2}A\eta^{1/2} - \frac{\kappa\rho_w}{3A}\eta^{-1/2}\ln\eta + \left(-\frac{2\kappa\rho_w}{3A} + \frac{B}{2}\right)\eta^{-1/2} + \cdots\right]. \tag{4.17}$$

Using (4.6) in (4.17), we further have

$$\begin{aligned} U^* = {} & \frac{3A}{2\rho_w}Y_*^{1/2} + \left[-\frac{\kappa}{3A}(-x_*)^{2/5} + \cdots\right]\frac{\ln Y_*}{Y_*^{1/2}} \\ & + \left[\frac{2\kappa}{15A}(-x_*)^{2/5}\ln(-x_*) + \left(-\frac{2\kappa}{3A} + \frac{B}{2\rho_w}\right)(-x_*)^{2/5} + \cdots\right]\frac{1}{Y_*^{1/2}} + \cdots. \end{aligned} \tag{4.18}$$

On the other hand, substituting (4.15) into (4.13*a*), we find

$$U^* = \frac{3A}{2\rho_w}Y_*^{1/2} + \frac{F(x_*)}{2\rho_w}\frac{\ln Y_*}{Y_*^{1/2}} + \frac{1}{\rho_w}\left[F(x_*) + \frac{1}{2}G(x_*)\right]\frac{1}{Y_*^{1/2}} + \cdots \quad \text{as} \quad Y_* \to \infty,$$

which, on being compared with (4.18), shows that

$$F(x_*) = -\frac{2\kappa\rho_w}{3A}(-x_*)^{2/5} + \cdots \quad \text{as} \quad x_* \to -\infty. \tag{4.19}$$

The corresponding formula for the pressure is obtained from matching with (2.61) as

$$P^*(x_*) = \kappa(-x_*)^{2/5} + \cdots \quad \text{as} \quad x_* \to -\infty. \tag{4.20}$$

Integrating (4.16) with initial conditions (4.19) and (4.20), we find

$$F(x_*) = -\frac{2\rho_w}{3A}P^*(x_*). \tag{4.21}$$

4.2. *Region* 4

The form of the asymptotic expansions of the fluid dynamics functions in the main part of the boundary layer (region 4) may be inferred by observing the behaviour of the solution in the overlapping region between regions 4 and 5 (see figure 12). Substituting (4.15) into (4.13) and then into (4.4) we find, using (4.10), that in the overlapping region

$$\begin{aligned} u' = {} & \frac{3A}{2\rho_w}Y^{1/2} + \sigma^{2/5}|\ln\sigma|\left[\frac{F(x_*)}{5\rho_w}\frac{1}{Y^{1/2}} + \cdots\right] \\ & + \sigma^{2/5}\left[\frac{F(x_*)}{2\rho_w}\frac{\ln Y}{Y^{1/2}} + \frac{F(x_*)}{\rho_w}\frac{1}{Y^{1/2}} + \frac{G(x_*)}{2\rho_w}\frac{1}{Y^{1/2}} + \cdots\right] + \cdots, \end{aligned}$$

$$v' = Re^{-1/2}\sigma^{-3/5}|\ln\sigma|\left[-\frac{2}{5\rho_w}F'(x_*)Y^{1/2}+\cdots\right] + Re^{-1/2}\sigma^{-3/5}\left[-\frac{F'(x_*)}{\rho_w}Y^{1/2}\ln Y - \frac{G'(x_*)}{\rho_w}Y^{1/2}+\cdots\right]+\cdots.$$

This suggests that the solution in region 4 should be sought in the form

$$\left.\begin{aligned} u'(x', y'; Re) &= U_{00}(Y) + \sigma^{2/5}|\ln(\sigma)|\,\tilde U_1(x_*, Y) + \sigma^{2/5}\tilde U_2(x_*, Y)+\cdots,\\ v'(x', y'; Re) &= Re^{-1/2}\sigma^{-3/5}|\ln(\sigma)|\,\tilde V_1(x_*, Y) + Re^{-1/2}\sigma^{-3/5}\tilde V_2(x_*, Y)+\cdots,\\ \rho(x', y'; Re) &= R_{00}(Y) + \sigma^{2/5}|\ln(\sigma)|\,\tilde R_1(x_*, Y) + \sigma^{2/5}\tilde R_2(x_*, Y)+\cdots,\\ h(x', y'; Re) &= h_{00}(Y) + \sigma^{2/5}|\ln(\sigma)|\,\tilde h_1(x_*, Y) + \sigma^{2/5}\tilde h_2(x_*, Y)+\cdots,\\ \mu(x', y'; Re) &= \mu_{00}(Y) + \sigma^{2/5}|\ln(\sigma)|\,\tilde\mu_1(x_*, Y) + \sigma^{2/5}\tilde\mu_2(x_*, Y)+\cdots,\\ p(x', y'; Re) &= \sigma^{2/5}\tilde P_1(x^*, Y)+\cdots, \end{aligned}\right\} \tag{4.22}$$

where functions $U_{00}(Y)$ and $\tilde V_1(x_*, Y)$ are such that

$$\left.\begin{aligned} U_{00}(Y) &= \frac{3A}{2\rho_w}Y^{1/2}+\cdots\\ \tilde V_1(x_*, Y) &= -\frac{2}{5\rho_w}F'(x_*)Y^{1/2}+\cdots \end{aligned}\right\} \quad \text{as} \quad Y\to 0. \tag{4.23}$$

Substitution of (4.22) into the Navier–Stokes equations yields

$$U_{00}(Y)\frac{\partial\tilde U_1}{\partial x_*} + \tilde V_1 U_{00}'(Y) = 0, \tag{4.24a}$$

$$\frac{\partial\tilde P_1}{\partial Y} = 0, \tag{4.24b}$$

$$U_{00}(Y)\frac{\partial\tilde h_1}{\partial x_*} + \tilde V_1 h_{00}'(Y) = 0, \tag{4.24c}$$

$$R_{00}(Y)\frac{\partial\tilde U_1}{\partial x_*} + U_{00}(Y)\frac{\partial\tilde R_1}{\partial x_*} + R_{00}(Y)\frac{\partial\tilde V_1}{\partial Y} + \tilde V_1 R_{00}'(Y) = 0, \tag{4.24d}$$

$$h_{00} = \frac{1}{(\gamma-1)R_{00}(Y)}, \qquad \tilde h_1 = -\frac{\tilde R_1}{(\gamma-1)[R_{00}(Y)]^2}. \tag{4.24e}$$

Substituting (4.24*e*) into the energy equation (4.24*c*), we find that

$$U_{00}(Y)\frac{\partial\tilde R_1}{\partial x_*} + \tilde V_1 R_{00}'(Y) = 0,$$

which, being combined with the continuity equation (4.24*d*), shows that the latter may be written in the form

$$\frac{\partial\tilde U_1}{\partial x_*} + \frac{\partial\tilde V_1}{\partial Y} = 0. \tag{4.25}$$

We use (4.25) to eliminate $\tilde U_1$ from the momentum equation (4.24*a*). We have

$$U_{00}(Y)\frac{\partial\tilde V_1}{\partial Y} - \tilde V_1 U_{00}'(Y) = 0,$$

or, equivalently,

$$\frac{\partial}{\partial Y}\left(\frac{\tilde V_1}{U_{00}}\right) = 0. \tag{4.26}$$

Equation (4.26) should be integrated with initial conditions (4.23), leading to

$$\frac{\tilde{V}_1}{U_{00}} = -\frac{4}{15A}F'(x_*).$$

Using the asymptotic expansions (4.22), we find that in region 4 the slope of the streamlines

$$\begin{aligned}\vartheta = \frac{v'}{u'} &= Re^{-1/2}\sigma^{-3/5}|\ln\sigma|\frac{\tilde{V}_1}{U_{00}} + \cdots \\ &= Re^{-1/2}\sigma^{-3/5}|\ln\sigma|\left[-\frac{4}{15A}F'(x_*)\right] + \cdots.\end{aligned} \tag{4.27}$$

4.3. *Region* 3

The flow in the upper tier (region 3 in figure 12) is governed by the transonic small perturbation theory. When analysing this flow, we shall use the Cartesian coordinates (x, y). Guided by (4.27) we introduce a small parameter,

$$\delta = Re^{-1/2}\sigma^{-3/5}|\ln\sigma| = \sigma^{3/5},$$

and expand the fluid dynamic functions in region 3 as

$$\left.\begin{aligned}u(x, y; Re) &= 1 + \delta^{2/3}u_1(x_*, y_*) + \delta^{4/3}u_2(x_*, y_*) + \cdots, \\ v(x, y; Re) &= \delta v_1(x_*, y_*) + \delta^2 v_2(x_*, y_*)\cdots, \\ p(x, y; Re) &= \delta^{2/3}p_1(x_*, y_*) + \delta^{4/3}p_2(x_*, y_*) + \cdots, \\ \rho(x, y; Re) &= 1 + \delta^{2/3}\rho_1(x_*, y_*) + \delta^{4/3}\rho_2(x_*, y_*) + \cdots, \\ h(x, y; Re) &= \frac{1}{\gamma - 1} + \delta^{2/3}h_1(x_*, y_*) + \delta^{4/3}h_2(x_*, y_*) + \cdots,\end{aligned}\right\} \tag{4.28}$$

with order-one independent variables defined as

$$x_* = \frac{x}{\sigma} = O(1), \qquad y_* = \frac{y}{\sigma\delta^{-1/3}} = O(1). \tag{4.29}$$

Substitution of (4.28), (4.29) into the Navier–Stokes equations yields in the leading-order approximation

$$\frac{\partial u_1}{\partial x_*} = -\frac{\partial p_1}{\partial x_*}, \tag{4.30a}$$

$$\frac{\partial v_1}{\partial x_*} = -\frac{\partial p_1}{\partial y_*}, \tag{4.30b}$$

$$\frac{\partial h_1}{\partial x_*} = \frac{\partial p_1}{\partial x_*}, \tag{4.30c}$$

$$\frac{\partial u_1}{\partial x_*} = -\frac{\partial \rho_1}{\partial x_*}, \tag{4.30d}$$

$$h_1 = -\frac{1}{\gamma - 1}\rho_1 + \frac{\gamma}{\gamma - 1}p_1. \tag{4.30e}$$

The far-field conditions for these equations follow from matching asymptotic expansions (4.28) with the solution (2.18), (2.19) and (2.21) in region 1. We have

$$\left.\begin{aligned} u_1 &= \frac{1}{\gamma+1} y_*^{1/2} F_0'(\xi) + \cdots \\ v_1 &= \frac{1}{\gamma+1} y_*^{3/4} \left[\tfrac{7}{4} F_0(\xi) - \tfrac{5}{4}\xi F_0'(\xi)\right] + \cdots \\ p_1 &= -\frac{1}{\gamma+1} y_*^{1/2} F_0'(\xi) + \cdots \end{aligned}\right\} \quad \text{as} \quad y_* \to \infty, \qquad (4.31a\text{–}c)$$

where

$$\xi = \frac{x_*}{y_*^{5/4}}.$$

Integration of the x-momentum (4.30a) and energy (4.30c) equations yields

$$u_1 = -p_1, \qquad h_1 = p_1. \qquad (4.32a, b)$$

Substituting (4.32b) into the state equation (4.30e), we further find that

$$\rho_1 = p_1. \qquad (4.33)$$

We see that $\rho_1 = -u_1$, which means that the continuity equation (4.30d) is satisfied automatically, leaving us with the y-momentum equation (4.30b). In view of the first of equations (4.32) it may be written in the form

$$\frac{\partial u_1}{\partial y_*} - \frac{\partial v_1}{\partial x_*} = 0. \qquad (4.34)$$

This equation, considered on its own, is not sufficient to determine the flow field in region 1, which is why we must turn to the second-order approximation.

The second-order equations are written as

$$\frac{\partial u_2}{\partial x_*} + (u_1 + \rho_1)\frac{\partial u_1}{\partial x_*} = -\frac{\partial p_2}{\partial x_*}, \qquad (4.35a)$$

$$\frac{\partial h_2}{\partial x_*} + (u_1 + \rho_1)\frac{\partial h_1}{\partial x_*} = \frac{\partial p_2}{\partial x_*} + u_1 \frac{\partial p_1}{\partial x_*}, \qquad (4.35b)$$

$$\frac{\partial}{\partial x_*}(u_2 + \rho_2 + \rho_1 u_1) + \frac{\partial v_1}{\partial y_*} = 0, \qquad (4.35c)$$

$$h_2 = \frac{1}{\gamma-1}\left(-\rho_2 + \rho_1^2\right) + \frac{\gamma}{\gamma-1}(p_2 - \rho_1 p_1). \qquad (4.35d)$$

Here we have omitted the y-momentum equation, as it will not be required for the analysis that follows.

Using (4.32) and (4.33), we can express equations (4.35) in the form

$$\frac{\partial u_2}{\partial x_*} = -\frac{\partial p_2}{\partial x_*}, \qquad (4.36a)$$

$$\frac{\partial h_2}{\partial x_*} = \frac{\partial p_2}{\partial x_*} - u_1 \frac{\partial u_1}{\partial x_*}, \qquad (4.36b)$$

$$\frac{\partial}{\partial x_*}\left(u_2 + \rho_2 - u_1^2\right) + \frac{\partial v_1}{\partial y_*} = 0, \qquad (4.36c)$$

$$h_2 = \frac{\gamma}{\gamma-1} p_2 - \left(\frac{1}{\gamma-1}\rho_2 + u_1^2\right). \qquad (4.36d)$$

Equations (4.36a) and (4.36b) are easily integrated to yield

$$u_2 = -p_2, \qquad h_2 = p_2 - \tfrac{1}{2}u_1^2. \tag{4.37a,b}$$

Equation (4.37b) is used to eliminate h_2 from (4.36d) to obtain

$$\rho_2 = p_2 - \tfrac{1}{2}(\gamma - 1)u_1^2. \tag{4.38}$$

Combining (4.38) with (4.37a), we have

$$u_2 + \rho_2 = -\frac{1}{2}(\gamma - 1)u_1^2,$$

substitution of which into the continuity equation (4.35c) leads to the Kármán–Guderley equation

$$(\gamma + 1)u_1 \frac{\partial u_1}{\partial x_*} - \frac{\partial v_1}{\partial y_*} = 0. \tag{4.39}$$

It should be considered together with the zero vorticity equation (4.34).

The far-field boundary conditions for the set of equations (4.39) and (4.34) are given by (4.31a,b). In order to close the problem, we must also formulate the matching condition with the solution in the main part of the boundary layer (region 4 in figure 12). According to (4.28), the slope of the streamlines in region 3

$$\vartheta = \frac{v}{u} = \delta v_1(x_*, y_*) + \cdots.$$

This, being compared with (4.27), shows that

$$v_1\Big|_{y_*=0} = -\frac{4}{15A}F'(x_*).$$

Here, function $F(x_*)$ is related to the pressure $P^*(x_*)$ acting in the boundary layer via equation (4.21). Hence,

$$v_1\Big|_{y_*=0} = \frac{8\rho_w}{45A^2}\frac{\mathrm{d}P^*}{\mathrm{d}x_*}. \tag{4.40}$$

Since the pressure does not change across regions 4 and 5, we can deduce, by comparing the asymptotic expansions for pressure in (4.4) and (4.28), that

$$p_1\Big|_{y_*=0} = P^*(x_*).$$

Finally, using (4.32a), we can express (4.40) in the form

$$v_1 = -\frac{8\rho_w}{45A^2}\frac{\partial u_1}{\partial x_*} \quad \text{at} \quad y_* = 0. \tag{4.41}$$

This completes the formulation of the interaction problem.

4.4. *Interaction problem*

For further discussion, it is convenient to introduce the velocity potential $\phi_1(x_*, y_*)$ such that

$$u_1 = \frac{1}{\gamma + 1}\frac{\partial \phi_1}{\partial x_*}, \qquad v_1 = \frac{1}{\gamma + 1}\frac{\partial \phi_1}{\partial y_*}. \tag{4.42}$$

The existence of this function follows from the zero vorticity equation (4.34).

With (4.42), the Kármán–Guderley equation (4.39) takes the form

$$\frac{\partial \phi_1}{\partial x_*}\frac{\partial^2 \phi_1}{\partial x_*^2} - \frac{\partial^2 \phi_1}{\partial y_*^2} = 0. \tag{4.43}$$

It should be solved with the condition of interaction with the boundary layer (4.41),

$$\frac{\partial \phi_1}{\partial y_*} = -\frac{8\rho_w}{45A^2}\frac{\partial^2 \phi_1}{\partial x_*^2} \quad \text{at} \quad y_* = 0, \tag{4.44}$$

and the far-field boundary condition (4.31) which, being in terms of ϕ_1, has the form

$$\phi_1 = y_*^{7/4} F_0(\xi) + \cdots \quad \text{as} \quad y_* \to \infty. \tag{4.45}$$

It should be noted that function $F_0(\xi)$ in (4.45) is not uniquely defined. It depends on choice of the group constant Λ in (2.30) or, equivalently, on the value of coefficient d_0 in the asymptotic formula (2.23). This arbitrariness reflects the fact that the flow in the interaction region depends on the nature of the inviscid flow outside this region. Still, it is easily seen that all transonic flows accelerating into a Prandtl–Meyer expansion fan are similar to one another. The similarity rule is expressed by the affine transformations

$$\phi_1 = \varkappa^{7/6} d_0^{5/12} \varphi, \quad x_* = \varkappa^{5/6} d_0^{-5/12} x, \quad y_* = \varkappa^{2/3} d_0^{-5/6} y,$$

where $\varkappa = 8\rho_w/45A^2$. Note that here in after x and y represent the canonical variables.

These transformations reduce the interaction problem (4.43)–(4.45) to the following canonical form. They leave equation (4.43) unchanged,

$$\frac{\partial \varphi}{\partial x}\frac{\partial^2 \varphi}{\partial x^2} - \frac{\partial^2 \varphi}{\partial y^2} = 0, \tag{4.46a}$$

while simplifying the interaction condition (4.44) to

$$\frac{\partial \varphi}{\partial y} = -\frac{\partial^2 \varphi}{\partial x^2} \quad \text{at} \quad y = 0. \tag{4.46b}$$

The far-field boundary condition (4.45) also preserves its form

$$\varphi = y^{7/4} F_0(\xi) + \cdots \quad \text{as} \quad y \to \infty, \quad \xi = \frac{x}{y^{5/4}} = O(1), \tag{4.46c}$$

but now function $F_0(\xi)$ is uniquely defined. It should be calculated by solving equation (2.22) subject to initial condition (2.31) for $k = 5/4$.

4.5. *Finite-distance singularity*

One of the main motivations for developing the theory of viscous–inviscid interaction was the need to describe the upstream influence in transonic and supersonic flows. During the 1940s and 1950s many experimentalists and theoreticians were involved in discussions of this phenomenon (see, for example, Chapman, Kuehn & Larson 1956). The first theoretical explanation of the upstream influence was given by Lighthill (1953). In the case of a supersonic boundary-layer flow, he demonstrated that if a perturbation is introduced in the boundary layer near point $x = 0$, then it would propagate upstream of this point with the pressure decaying as

$$p = Ce^{Kx} + \cdots \quad \text{as} \quad x \to -\infty. \tag{4.47}$$

Here Lighthill's solution is expressed in the notations of the viscous–inviscid interaction problem (1.2)–(1.5), (1.6*a*) which, of course, was formulated sixteen years later. Factor C in (4.47) depends on the nature and magnitude of the perturbation introduced into the boundary layer, whereas $K > 0$ is a universal constant which depends on the free-stream Mach number and the skin friction in the boundary layer immediately upstream of the interaction region.

On writing $C = \mathrm{sign}(C)\exp(Kx_s)$, $x_s = K^{-1}\ln|C|$, (4.47) takes the form

$$p = \mathrm{sign}(C)\exp(K(x + x_s)),$$

signifying that (apart from an arbitrary shift x_s along the body surface) the interaction problem (1.2)–(1.5), (1.6*a*) admits two types of solution. The first one corresponds to $\mathrm{sign}(C) > 0$ when the pressure grows in the boundary layer causing it to separate at some point on the body surface. The second solution, $\mathrm{sign}(C) < 0$, corresponds to the self-induced acceleration of the flow in the interaction region which terminates by a singularity at a finite point $x = x_0$. Neiland & Sychev (1966) and Neiland (1969*b*) were the first to describe this singularity in their analysis of the supersonic flow accelerating into a Prandtl–Meyer fan.

The transonic flow considered in this paper is also expected to undergo a monotonic acceleration along the wall, leading to a singularity at a finite point on the body contour. To determine the form of this singularity, we shall write equation (4.46*a*) in the form

$$u\frac{\partial u}{\partial x} - \frac{\partial v}{\partial y} = 0, \qquad \frac{\partial u}{\partial y} - \frac{\partial v}{\partial x} = 0, \tag{4.48}$$

where

$$u = \frac{\partial \varphi}{\partial x}, \qquad v = \frac{\partial \varphi}{\partial y}.$$

In a region where the longitudinal velocity component u is positive (which is certainly the case near the singularity) the set of equations (4.48) is hyperbolic. It has two families of characteristics. The first one is defined by the equation

$$\frac{\mathrm{d}y}{\mathrm{d}x} = \frac{1}{\sqrt{u}},$$

with the corresponding Riemann invariant being

$$\tfrac{2}{3}u^{3/2} - v = \zeta. \tag{4.49}$$

Similarly, on the characteristics of the second family

$$\frac{\mathrm{d}y}{\mathrm{d}x} = -\frac{1}{\sqrt{u}}, \qquad \tfrac{2}{3}u^{3/2} + v = \eta. \tag{4.50a,b}$$

Parameter ζ in (4.49) remains constant along each characteristic, but might be different for different characteristics, and is expected to grow with the flow acceleration. Contrary to that, parameter η in (4.50) remains finite. Indeed, according to (4.50*a*), the characteristics of the second family take their origin in the upstream flow field where u and v are finite, making η finite. Hence, when the velocity components u and v become large on approach to the singularity, η may be disregarded in (4.50*b*), reducing it to

$$\tfrac{2}{3}u^{3/2} + v = 0. \tag{4.51}$$

In particular, equation (4.51) may be considered on the wall where, according to (4.46*b*),

$$v = -\frac{\partial u}{\partial x}. \tag{4.52}$$

Eliminating v from (4.51) and (4.52), we have

$$\tfrac{2}{3}u^{3/2} = \frac{\partial u}{\partial x} \quad \text{at} \quad y = 0.$$

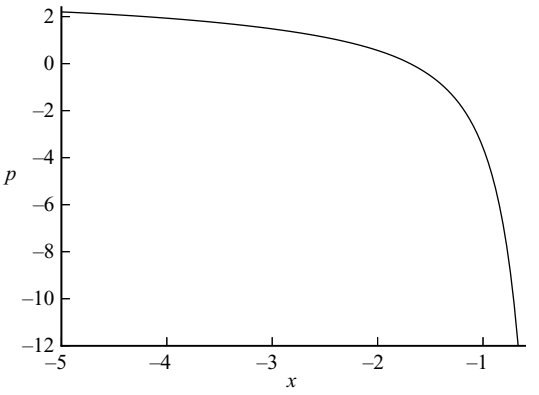

FIGURE 13. The pressure distribution in the interaction region.

This equation is easily integrated to give

$$u\Big|_{y=0} = \frac{9}{(x_0 - x)^2} + \cdots \quad \text{as} \quad x \to x_0^-. \tag{4.53}$$

Here, the constant of integration is denoted by x_0 to show that it represents the position of the singularity on the body contour. Since the boundary-value problem (4.46) is invariant with respect to an arbitrary shift in the x-direction, we can choose $x_0 = 0$ in (4.53).

4.6. *Numerical solution of the interaction problem*

In order to construct the solution to the interaction problem (4.46), we used a numerical scheme which employs finite differencing in the x-direction and a Chebyshev collocation method in the y-direction. The x-derivatives in the Kármán–Guderley equation (4.46*a*) were approximated in the same way as in the Murman & Cole (1971) scheme; see also Cole & Cook (1986). For the derivative $\partial^2\varphi/\partial x^2$ on the right-hand side of the interaction law (4.46*a*), the central differencing was used to allow the solution to account for upstream propagation of the perturbations. The y-derivatives in both the Kármán–Guderley equation (4.46*a*) and interaction law (4.46*b*) were evaluated with the help of the Chebyshev collocation method; see, for example, Canuto *et al.* (1988). The resulting set of nonlinear algebraic equations was solved using the Newton–Rhapson iteration.

The results of the calculations are shown in figure 13 in the form of pressure $p = -\partial\varphi/\partial x$ distribution along the body contour. Various grids were used, and it was found that with 40 Chebyshev polynomials and 150 points in the x-direction, the results are correct to four significant figures. The difference between the numerical results and asymptotic formula (4.53) reaches 1% at $x = -0.46$, and then diminishes further as $x \to 0^-$.

The singularity (4.53) is identical to the one encountered by Neiland & Sychev (1966) and Neiland (1969*b*) in their study of the supersonic flow over a sharp bend, say, a convex corner on the body contour. Assuming the Reynolds number to be large, they used the Prandtl–Meyer solution for the inviscid part of the flow outside the boundary layer. When passing through the Prandtl–Meyer expansion fan, the pressure of the gas in this region falls by an order-one amount, i.e.

$$\Delta p = O(1). \tag{4.54}$$

In the triple-deck region upstream of the corner

$$\Delta p = O(Re^{-1/4}). \tag{4.55}$$

Obviously, matching between (4.54) and (4.55) is only possible if the solution of the triple-deck problem upstream of the corner develops a singularity like (4.53).

Neiland & Sychev (1966) and Neiland (1969*b*) gave a detailed description of the flow behaviour in the $O(Re^{-1/2}) \times O(Re^{-1/2})$ region around the corner point as well as downstream of this region. When the transonic flow undergoes acceleration through (4.53), its behaviour becomes indistinguishable from that in the corresponding supersonic flow. As a result, the theory of Neiland & Sychev (1966) and Neiland (1969*b*) appears to be directly applicable to the flow considered in this paper.

5. Conclusions

In this paper we analysed, first of all, the inviscid transonic flow near a corner point O where the body contour is defined by equation (2.14). We found that for $1 < \alpha < 8/5$ the solution is influenced by the body shape both upstream and downstream of corner point O in figure 4 despite the downstream part of this flow being supersonic for $\alpha > 3/2$. As soon as parameter α reaches its critical value of $\alpha = 8/5$, the solution is found to represent a flow that undergoes very fast acceleration to form a Prandtl–Meyer fan. The latter blocks upstream propagation of the perturbations. As a result the flow field 'freezes', in the sense that it can no longer change with further bending of the body contour downstream of point O. This suggests that the inviscid transonic flow may accelerate into a Prandtl–Meyer expansion fan, not only when the gas moves over a convex corner (as it happens in supersonic flows), but also for a wider class of body shapes. The solution in the limiting case with $\alpha = 8/5$ is applicable to these situations.

Then the reaction of the boundary layer to the singular behaviour of the pressure gradient in the Prandtl–Meyer solution was analysed. We found that the Prandtl–Meyer flow represents one more example of unusual behaviour of transonic flows in the viscous–inviscid interaction region. Their distinctive nature is revealed, most notably, in the formulation of the interaction problem (4.46), which proves to be quite different from that in the corresponding supersonic and subsonic flows (1.1)–(1.6). In the study of the transonic viscous–inviscid interaction, the main difficulty lies in the calculation of the inviscid flow in the upper tier, where the nonlinear Kármán–Guderley equation (4.46*a*) should be solved. In the supersonic and subsonic flows, the solution in the upper tier is linear, leading to the interaction relations given by the Ackeret formula (1.6*a*) and Hilbert integral (1.6*b*), respectively. These are coupled with boundary-layer equations. In contrast, in the present transonic problem, we need not solve the boundary-layer equations (1.1)–(1.2); instead, the influence of the boundary layer is expressed through a simple boundary condition (4.46*b*) for the inviscid flow. In this respect, the transonic interaction problem considered here is similar to the incompressible boundary-layer separation on a moving wall (see Sychev 1984).

The reason for this difference is that transonic flow is capable of producing an extreme pressure gradient that acts on the boundary layer before the interaction region. In particular, in the transonic flow expanding into a Prandtl–Meyer fan, the pressure gradient is expressed by equation (3.6), i.e.

$$\frac{\mathrm{d}p}{\mathrm{d}x} = -\frac{2}{5}\frac{\kappa}{(-x)^{3/5}} + \cdots \quad \text{as} \quad x \to 0^-. \tag{5.1}$$

It is weaker than the pressure gradient (1.8) observed in transonic flow separating from a convex corner (Ruban & Turkyilmaz 2000), but stronger as compared to the pressure gradient (1.7) in the analogous subsonic flow (Ruban 1974).

As a result of the action of the pressure gradient (5.1), the gas in the boundary layer experiences an extreme acceleration. This changes the velocity profile across the boundary layer. In particular, near the wall, instead of being a linear function of Y, it behaves as $U \sim Y^{1/2}$; see (3.28). An 'inspection analysis' presented in Appendix B of Ruban & Turkyilmaz (2000) suggested that under these conditions the contribution of the viscous sublayer (region 5 in figure 12) would be comparable with that of the main part of the boundary layer (region 4). However, a more detailed analysis presented in this paper shows that the solution develops a logarithmic behaviour (4.15) at the outer edge of the viscous sublayer, which determines the displacement effect of the boundary layer. It therefore may be said that the main contribution to the displacement thickness is produced by the overlapping region that lies between the viscous sublayer (region 5) and main part of the boundary layer (region 4).

The theory of the boundary-layer separation in transonic flows is still in its infancy. Many important questions remain unanswered. Of particular interest is the question of why the shock wave, closing the local supersonic region on the upper surface of a wing, is observed to start oscillating as soon as it becomes strong enough to cause the boundary-layer separation. Another problem to consider concerns the turbulent boundary-layer separation at transonic speed. Does the dominance of the inviscid processes in the interaction region imply that the turbulent boundary-layer separation proceeds in a way that is similar to the laminar boundary-layer separation?

REFERENCES

Buldakov, E. V. & Ruban, A. I. 2002 On transonic viscous-inviscid interaction. *J. Fluid Mech.* **470**, 291–317.

Canuto, C., Hussaini, M. Y., Quarteroni, A. & Zang, T. A. 1988 *Spectral Methods in Fluid Dynamics*. Springer.

Chapman, D. R., Kuehn, D. M. & Larson, H. K. 1956 Investigation of separated flows in supersonic and subsonic streams with emphasis on the effect of transition. *NACA Rep.* 1356.

Cherny, G. G. 1988 *Gas Dynamics*. Nauka, Moscow.

Cole, J. D. & Cook, L. P. 1986 *Transonic Aerodynamics*. North-Holland.

Diyesperov, V. N. 1994 Some solutions of Kármán's equation describing the transonic flow past a corner point on a profile with a curvilinear generatrix. *Prikl. Mat. Mekh.* **58** (6), 68–77.

Guderley, K. G. 1948 Singularities at the sonic velocity. *Wright–Patterson AFB Rep. F-TR*-1171-*ND*.

Jenson, R., Burggraf, O. R. & Rizzetta, D. P. 1975 Asymptotic solution for supersonic viscous flow past a compression corner. *Lecture Notes in Physics* vol. 35, pp. 218–224. Springer.

Kirchhoff, G. 1869 Zur theorie freier flüssigkeitsstrahlen. *J. Reine Angew. Math.* **70** (4), 289–298.

Korolev, G. L. 1991 Asymptotic theory of laminar flow separation at a corner with small turning angle. *Izv. Akad. Nauk SSSR, Mech. Zhid. i Gaza* (1), 180–182.

Korolev, G. L. 1992 On the non-uniqueness of separated flow around corners with small turning angle. *Izv. Akad. Nauk SSSR, Mech. Zhid. i Gaza* (3), 178–180.

Korolev, G. L., Gajjar, J. S. B. & Ruban, A. I. 2002 Once again on the supersonic flow separation near a corner. *J. Fluid Mech.* **463**, 173–199.

Liepmann, H. W. & Roshko, A. 1957 *Elements of Gasdynamics*. Wiley.

Lighthill, M. J. 1953 On boundary layers and upstream influence. II. Supersonic flows without separation. *Proc. R. Soc. Lond.* A **217**, 478–507.

Messiter, A. F. 1970 Boundary-layer flow near the trailing edge of a flat plate. *SIAM J. Appl. Maths* **18**, 241–257.

Murman, E. M. & Cole, J. D. 1971 Calculation of plane steady transonic flows. *AIAA J.* **9**, 114–121.

Neiland, V. Ya. 1969*a* Theory of laminar boundary layer separation in supersonic flow. *Izv. Akad. Nauk SSSR, Mech. Zhid. i Gaza* (4), 53–57.

Neiland, V. Ya. 1969*b* Asymptotic theory of heat transfer calculation near a corner. *Izv. Akad. Nauk SSSR, Mech. Zhid. i Gaza* (5), 53–60.

Neiland, V. Ya. & Sychev, V. V. 1966 Asymptotic solutions of the Navier–Stokes in regions of large local perturbations. *Izv. Akad. Nauk SSSR, Mech. Zhid. i Gaza* (4), 43–49.

Prandtl, L. 1904 Über flüssigkeitsbewegung bei sehr kleiner Reibung. In *Verh. III. Intern. Math. Kongr., Heidelberg*, pp. 484–491. Teubner, Leipzig, 1905.

Ruban, A. I. 1974 Laminar separation from a corner point of a rigid body contour. *Uch. zap. TsAGI* **5** (2), 44–54.

Ruban, A. I. 1976 On the theory of laminar flow separation from a corner point on a solid surface. *Uch. zap. TsAGI* **7** (4), 18–28.

Ruban, A. I. & Turkyilmaz, I. 2000 On laminar separation at a corner point in transonic flow. *J. Fluid Mech.* **423**, 345–380.

Stewartson, K. 1969 On the flow near the trailing edge of a flat plate. *Mathematika* **16**, 106–121.

Stewartson, K. 1970 On laminar boundary layers near corners. *Q. J. Mech. Appl. Maths* **23**, 137–152.

Stewartson, K. & Williams, P. G. 1969 Self-induced separation. *Proc. R. Soc. Lond.* A **312**, 181–206.

Sychev, V. V. 1984 On the asymptotic theory of laminar separation from a moving surface. *Prikl. Math. Mech.* **48**, 247–253.

Vaglio-Laurin, R. 1960 Transonic rotational flow over a convex corner. *J. Fluid Mech.* **9**, 81–103.

Van Dyke, M. 1982 *An Album of Fluid Motion.* Parabolic.